UNIVERSITY OF CINCINNATI

DATE: November 13, 2002

I, Peter W. Soltys ,

hereby submit this as part of the requirements for the degree of:

Master of Science

in:

Geology

It is entitled:

GROUNDWATER FLOW MEASUREMENT IN A SINGLE WELL USING FLUOROMETER ANALYSIS OF DISPERSED AND ADSORBED FLUORESCEIN DYE

Approved by:

Dr. David B. Nash

Dr. Thomas V. Lowell

Dr. J. Barry Maynard

GROUNDWATER FLOW MEASUREMENT IN A SINGLE WELL USING FLUOROMETER ANALYSIS OF DISPERSED AND ADSORBED FLUORESCEIN DYE

A thesis submitted to the

Division of Research and Advanced Studies
of the University of Cincinnati

in partial fulfillment of the
requirements for the degree of

MASTER OF SCIENCE

in the Department of Geology
of the McMicken College of Arts and Sciences

2002

by

Peter W. Soltys

B.S. Pennsylvania State University, 1977
M.S. University of Pittsburgh, 1980

Committee Chair: Dr. David B. Nash

GROUNDWATER FLOW MEASUREMENT IN A SINGLE WELL USING FLUOROMETER ANALYSIS OF DISPERSED AND ADSORBED FLUORESCEIN DYE

By Peter W. Soltys

Abstract

This paper describes the development of a testing technique to determine groundwater flow direction and velocity in a single well. A series of experiments were performed using a device designed specifically to fit into a 152.4 mm (6 inch) diameter well casing. A test apparatus was assembled of polyvinyl chloride (PVC) pipes using porous stones to simulate groundwater flow conditions in an aquifer. The measurement device released fluorescein dye into the center of the simulated well using a dye release mechanism consisting of a glass vial with a salt plug suspended in modeling clay at its base. A small hole in exposed the top and bottom of the salt plug allowed the exchange of dye with the groundwater flowing past the dye outlet hole. The dye released into the well was subsequently adsorbed onto the surface of carbon rods located at eight equally spaced points around the perimeter of the well. The relative amount of the fluorescein dye remaining in the dye release vial, as well as the amount adsorbed on the carbon rods, was measured by the intensity of fluorescence detected by a fluorometer. The amount of the dye adsorbed onto the rods was shown to indicate the direction of groundwater flow with low directional dispersion. Groundwater flow velocity measurements were attempted using two methods. The first method correlated the fluorometer reading for the fluorescein dye/groundwater mixture remaining in the vial after a measured period of time with the flow velocity. The second method correlated the root-mean-square of the fluorometer readings for the fluorescein dye adsorbed onto and extracted from the carbon rods for an individual experiment with the groundwater flow velocity. The results of the first method's groundwater flow velocity experiments were a set of linear equations based on a multiple linear regression analysis relating discharge, measurement time, and fluorometer readings. The second method resulted in a linear relationship between the groundwater flow velocity and the root-mean-square of the carbon rod adsorption data. However, the groundwater flow velocity analysis using both methods showed poor correlation coefficients for the derived linear relationships. The suspect groundwater

velocity measurements were attributed to the inconsistent nature of the dye release process and the inherent problems of introducing a dye tracer into a low Reynolds number laminar flow environment.

AKNOWLEDGEMENTS

I wish to acknowledge the U.S. Geological Survey, Water Resources Division, Columbus, Ohio, for their help in obtaining several of the references used in this thesis and for the use of their fluorometer for the analysis of the samples described in this thesis. I also wish to thank the Department of Geology at the University of Cincinnati, especially Dr. David B. Nash, for keeping my wonder of geology alive. Lastly, I wish to thank Connie for her understanding and support and Gabrielle and Rachel for their enthusiasm during my graduate work.

GROUNDWATER FLOW MEASUREMENT IN A SINGLE WELL USING FLUOROMETER ANALYSIS OF DISPERSED AND ADSORBED FLUORESCEIN DYE

TABLE OF CONTENTS

Table of Contents 1

List of Tables 2

List of Figures 3

List of Symbols 4

Introduction 6

Background 8

Advantages of Fluorescein Dye Adsorption and Dilution Technique 13

Measurement Theory 14

Groundwater Flow Simulation 15

Measurement Device 21

Dye Release Vial Preparation 25

Experiment Procedure 27

Observations 30

Results 35

- Groundwater Flow Direction Results 35
- Groundwater Flow Velocity Results 42

Conclusions 48

Bibliography 51

LIST OF TABLES

Table No.	Title	Page
1	Groundwater Flow Direction Analysis Carbon Rod Fluorometer Results	36
2	Directional Data Analysis of Maximum Fluorometer Reading Vectors	38
3	Summary of X^2 Calculations for Each Flow Direction Test	41
4	Groundwater Velocity Analysis Fluorometer Results	44
5	Groundwater Flow Velocity Analysis Using Root-Mean-Squares and Carbon Rod Fluorometer Results	47

LIST OF FIGURES

Figure No.	Title	Page
1	Test apparatus with manometers removed to show well pipe	16
2	Test apparatus configured for flow velocity and direction measurement. A second (lower) drain line is located on the backside and near the base of the outlet standpipe. Both drain lines discharge into the sink	17
3	Porous stone and adapter ring assembly	19
4	Porous stone/adapter ring assembly installed in PVC pipe coupling	19
5	Manometer display board showing differential water levels in the manometers during a groundwater flow experiment	20
6	Illustration of the groundwater flow direction and velocity measurement device with oblique views looking (a) down and (b) up	22
7	Cut-away illustration of the dye release vial	26
8	Dye release vial with modeling clay/salt plug in place. Note hole in top of modeling clay	26
9	Groundwater flow direction and velocity measurement device (a) prepared for insertion in the simulated well with the bottom of the dye release vial and salt plug protected by a No. 4 rubber stopper, and (b) with dye release vial in position to expose salt plug to water	28
10	View through the groundwater flow direction and velocity measurement device window showing the salt density current before the start of the fluorescein dye release	32
11	Angled view through the front window of the test apparatus showing the fluorescein dye stream. The view is angled to provide contrast to reveal the dye stream in the photograph	33
12	Sketch of fluorescein dye stream illustrating the progressive formation of globule, cup, and donut-shaped features as the dye thread disintegrates	34
13	Flow direction roses normalized to the individual test maximum flow. Flow was introduced into the test chamber from the south and exited to the north. The numbers next to the compass points refer to the carbon rod positions on the test device	37
14	Multiple-regression analysis results for the fluorescein dye concentration in the test release vial	45
15	Plot of RMS values derived from the carbon rod fluorometer readings versus groundwater velocity.	48

LIST OF SYMBOLS

Symbol	Definition
A	Cross-sectional area, mm^2 (ft^2)
D	Pipe diameter in mm or m (ft)
f	Fluorometer reading
i	Location number of carbon rod; counter
J, K, L	Constants
j	Counter for bins
k	Number of probability intervals (bins)
n	Porosity of the porous medium; Total number of carbon rods
m	Number of probability intervals (bins)
P	Probability
p	Number of evaluation parameters used to define probability distribution
Q	Groundwater discharge, ml/s (ft^3/s)
R	Reynolds number; Resultant vector length
$\overline{R}$	Mean resultant length
r_i	Ratio of fluorometer reading for carbon rod i to the mean of the fluorometer readings for all carbon rods in a single experiment
r^2	Correlation coefficient
RMS	Root-mean-square
t	Time, min
V, v	Average water velocity, mm/s or m/s (ft/s)
v^*	Apparent groundwater velocity, ml/s (ft/s)
X_r	X-component of the vector resultant
$\overline{x}$	Mean of carbon rod fluorometer readings for a single experiment

LIST OF SYMBOLS (cntd.)

Symbol	Definition
x_i	Fluorometer reading for carbon rod *i* as percent of total readings for an experiment; fluorometer reading for carbon rod *i*
x_n	Normal square deviation for carbon rod fluorometer readings used in Chi-Square analysis
Y_r	Y-component of the vector resultant
α	Groundwater focusing or well-shape factor
X^2	Chi-squared test statistic
μ	Absolute viscosity of water kg/m·s (lb·s/ft^2)
ν	Degrees of freedom
θ_i	Bearing angle of the carbon rod at location i
$\bar{\theta}$	Mean direction of the resultant vector
ρ	Density of water in kg/m^3 (slug/ft^3)

GROUNDWATER FLOW MEASUREMENT IN A SINGLE WELL USING FLUOROMETER ANALYSIS OF DISPERSED AND ADSORBED FLUORESCEIN DYE

By Peter W. Soltys

Introduction

The measurement of groundwater flow direction and magnitude is useful in a variety of environmental, water resources and geotechnical engineering investigations including the determination of contaminant migration and source identification, groundwater resource availability, water budget analysis, and foundation analysis. Currently, the methodologies developed to determine the direction and magnitude of groundwater flow are generally divided into indirect methods (e.g. monitoring well networks) and direct methods (e.g. in-hole measurements).

The use of monitoring wells to locate the extent of a contaminant plume based on the concentration of the contaminant detected or to track a tracer element introduced into a well is somewhat simple to implement. However, the cost of drilling monitoring wells and securing easements or permission to drill from adjacent property owners as well as the cost of the drilling itself can be prohibitive. Usually, the indirect measurement of groundwater discharge is accomplished by obtaining the piezometric elevation in at least three wells, determining the gradient, performing a pump test to estimate hydraulic conductivity, and indirectly calculating the velocity from the measurements. Depending on the aquifer material, monitoring wells can also involve lengthy monitoring periods and large amounts of tracer in order to establish the velocity and direction of groundwater flow.

In-hole groundwater flow measurement techniques can also provide accurate groundwater direction and flow measurements. For many groundwater investigations, direct measurement techniques can eliminate or significantly reduce the number of wells that are needed to evaluate groundwater flow and direction. It should be noted that in-hole groundwater flow measurements must take into account the increased

groundwater flow velocity within the open well cavity as opposed to the permeable aquifer material. To date, there have been a variety of instruments used to directly measure groundwater flow velocity and direction including in situ permeable flow sensors, charged-couple device cameras, and heat-pulse flow meters. Although these instruments have shown varying degrees of success in measuring groundwater flow and velocity, they have also proven to be expensive, delicate, and dependent on a reliable electrical power source at the testing site for both the instrument and the aboveground monitoring and data recording devices.

The purpose of this project was to develop a groundwater flow direction and magnitude measurement device for groundwater measurement in a single well that was inexpensive and simple to operate and robust enough to withstand the rigors of testing in remote areas. This thesis describes a fluorescent dye detection methodology for groundwater measurement using an instrument and test apparatus developed and assembled by the author.

Fluorescein dye has been used since 1877 to trace groundwater flow ("The First Fluorescent," n.d.) and has been widely used to study solute-transport characteristics of groundwater in karst terranes (Mull et al., 1988). In karst studies, the fluorescein dye is brought to an injection point such as a swallet or plugged sinkhole, poured onto the ground, and infiltrates into the aquifer. The U.S. Geological Survey (USGS) attempts to limit the maximum concentration of fluorescein dye at the measurement point to 0.01 mg/l (Hubbard et al., 1982). The recommended amount of fluorescein disodium salt ($C_{20}H_{10}O_5Na_2$) used in karst studies usually varies between 0.23 kg and 0.46 kg (0.5 lb and 1.0 lb) per straight-line mile of trace up to a maximum of 2.27 kg (5.0 lbs) (Quinlan, 1987 and Mull, et al., 1988a). The amount of water mixed with the fluorescein dye powder used in karst studies has varied from 1.9 kl to 6.1 kl (500 gal. to 1,600 gal.) (Mull et al., 1988). The fluorescein dye is then captured through adsorption onto charcoal suspended in a bag at the suspected groundwater resurgence points. The fluorescein dye is detected by soaking the charcoal in an alcohol solution and detecting the fluorescence in a fluorometer.

The instrument developed for this project also used carbon in the form of rods to capture fluorescein dye released into a well. However, the amount of fluorescein dye solution used in the experiments was much less, only 5 ml. Like the previously described karst studies, the fluorescein dye was released from the carbon rods by soaking the rods in alcohol (methanol) and then detecting the fluorescence in a fluorometer.

Background

The measurement of groundwater flow direction and velocity has been investigated using both direct measurement and indirect measurement techniques. These investigations have included groundwater flow measurements in a single well and groups of wells.

Direct measurement of groundwater flow velocity has involved a variety of in-borehole probes and aboveground instruments. The heat-pulse flow meter was originally developed by the U.S. Geological Survey to measure vertical flow in a well. The heat-pulse flow meter measures vertical flow by introducing a pulse of heated water in a well and measuring the arrival time for the peak temperature at a thermister sensor over a set distance. Kerfoot (1988) and Pailett et al. (1996) documented the use of heat-pulsing flow meters to measure groundwater flow. No cases have been documented where the heat-pulse flow meter has been used to directly measure horizontal groundwater flow velocity. A horizontal alignment of the heat-pulse flow meter to measure horizontal velocities would have to account for the turbulence caused by a thermally more buoyant plume of water that would be rising as well as moving in the downstream direction. The dispersion of the heated water plume in both the vertical and horizontal instrument alignments also need to be accounted for in the measurements. Other disadvantages of the heat-pulse flow meter include the need to provide electric power throughout the measurement phase to power the water heating unit and the thermistor sensors on the probe and the aboveground calibration, recording, and analysis equipment. The heat-pulse probe and aboveground support equipment are sensitive and subject to damage from normal handling in the field.

In a manner similar to the use of a heat-pulse flow meter, Wheatcraft (1986) measured temperature differences across a borehole due to advective fluid transport to estimate groundwater velocity and direction. Thermistor sensors were used by Wheatcraft to detect temperature differences across open space in a well, and the differences in temperature were calibrated to the groundwater velocity and direction in a large sand box flow chamber. Wheatcraft noted that direct groundwater flow velocity measurements could be made if the instrument was modified to output temperature breakthrough curves for all of the thermistors. Wheatcraft's experiments were conducted in a laboratory; however, field applications of this method of groundwater flow velocity and direction measurement will still require a reliable electrical power supply and involve sensitive equipment.

Momii et al. (1993) used laser Doppler velocimeters to measure groundwater flow based on the wavelength shift in reflected laser light beamed through a groundwater flow control section. Although this technology has been widely used to measure pressure flows in pipes where a uniform cross-section is readily available and the pipe is usually easy to access, in a borehole the control section and laser must be made part of the probe. The wavelength shift measured by the laser Doppler velocimeter is sensitive to the amount of sediment in the groundwater flow; therefore, the instrument must be installed for an adequate length of time to allow any sediment stirred up by the insertion of the probe in the borehole to settle. The amount of time necessary to allow the sediments to settle must be estimated and can lead to errors if an inadequate time was allotted before beginning the measurements. The use of a laser Doppler velocimeter again requires providing a reliable source of electrical power to the measurement site for the duration of the experiment for the probe and the supporting calibration, recording, and analysis equipment. Like the heat-pulse flow meter, the laser Doppler velocimeter and the aboveground components can sensitive to mishandling.

The magnitude of groundwater velocity has been estimated for naturally occurring particles in a well using a charged-couple device (CCD) camera (Kearl, 1997). Kearl reported flow velocities in semi-consolidated fine sand and silt of 3.6×10^{-3} cm/s (1.18×10^{-4} ft/s) to 1.2×10^{-2} cm/s (3.94×10^{-4} ft/s) in alluvial sands and gravels. Kearl's experiments were verified in a laminar flow chamber at the Desert Research Center in Boulder City, Nevada where it was found that after groundwater flow was disturbed in a well by the insertion of the CCD camera, laminar horizontal flow dominated after 20 to 30 minutes. The use of a CCD camera has also been applied to the measurement of both groundwater velocity and the vertical distribution of groundwater velocity (Yamada and Arakawa, 1999). In addition to the need for a reliable power source, use of a CCD requires a compass to align the probe, an optical magnification lens, and an illumination source. Once again, the probe and aboveground support equipment is relatively easy to damage.

The U.S. Department of Energy (USDOE, 1998) has used in situ permeable flow sensors (ISPFS) at the Savannah River Site, Aiken, South Carolina; the Hanford Site, Richland, Washington; and the Weeks Island Strategic Petroleum Reserve Site, Weeks Island, Louisiana, to determine groundwater flow velocity and direction. The ISPFS is a cylindrical heater with a diameter just smaller than a borehole. The sediments around the borehole collapse upon the heater as the drill casing is removed providing direct contact between the groundwater and the heater. A series of calibrated temperature sensors on the surface of the heater detect changes in the temperature field around the heater. Groundwater flow and direction can then be determined by changes in the temperature field as groundwater flows past the ISPFS. The ISPFS heats the groundwater and sediments surrounding the probe by 20ºC to 30ºC and requires approximately 80 watts of power to the heater. The work to develop the ISPFS technique was documented by Peterson et al. (1994), Ballard (1996), and Ballard et al. (1996). For one experiment conducted at the Savannah River Site where two ISPFS's were installed in a confined aquifer at distances of 5 m (16.4 ft) and 12 m (39.4 ft) from a monitoring well containing a submersible pump, the USDOE reported that the magnitude of velocity measured by the ISPFS's was linearly related to the pumping rate.

At the Hanford Site, ISPFS's installed to study the interaction between groundwater and the level of water in the Columbia River showed water flowing away from the river during high stages and towards the river during low stages. In general, the ISPFS was shown to accurately measure groundwater flow velocity in the range of approximately 5×10^{-6} to 5×10^{-3} cm/s (1.64×10^{-7} to 1.64×10^{-4} ft/s). The USDOE (1998) identified initial costs for an ISPFS of $7,550 with estimated annual costs of $1,000. Although the ISPFS has the advantages of being able to monitor groundwater flow and direction over a long period of time (estimated lifetime of at least 10 years) and providing three-dimensional flow velocity and direction data, a reliable electrical power source must be provided for the duration of the experiment. The USDOE also found that the creation of conduits around the perimeter of the ISPFS during installation could cause erroneous indications of downward directed flow, which must be addressed through the use of grout or bentonite material to seal the annulus. Any unusual results detected by the ISPFS must be investigated, which could include removal of the instrument from the borehole, checking the equipment, recalibration, and boring the hole again and installing casing, and reinstallation of the instrument, which adds to the overall cost of the groundwater monitoring program.

Indirect flow measurement techniques have included the evaluation of soil to determine the gradient of chlorine concentration in different layers of soil as an indicator of groundwater flow direction (Mizumura and Hasatani, 2001). Reiter (2001), drawing on the work of Stallman (1963), Bredehoeft and Papadopulos (1965), Mansure and Reiter (1979), Reiter and Mansure (1983), Reiter et al. (1989), McCord et al. (1992), and Lu and Ge (1996), has used precision temperature logs obtained from borings in Virginia and New Mexico, along with equations that have been derived to relate conductive heat flow to temperature, to estimate the horizontal and vertical components of groundwater velocity in a borehole. Precise temperature measurements were also used by Drury et al. (1981) to estimate groundwater flow velocity in boreholes. The use of temperature logs required the analysis of multiple curve equations to find the equation that best fit the data. The best-fit curve ultimately was shown to define a plane in three-dimensions defined by the depth of the water in the well, groundwater temperature, and temperature

gradient. The various coefficients used in the best-fit equation are adjusted to create a better fit for the data. The use of temperature logs was largely a mathematical exercise used to predict future groundwater flow velocities in the same borehole based on past data; therefore, there were no constraining groundwater flow velocities identified. In each of these techniques, data from multiple wells was required with the associated costs of drilling and data gathering.

Sébastien et al. (2002) conducted point dilution tests to estimate groundwater velocity. In this technique a solution of KCl was injected into a well and the change of electrical conductivity of the water in the well with time was determined to be proportional to the groundwater velocity. Groundwater velocities in the range 1.39×10^{-4} to 1.11×10^{-2} cm/s (4.56×10^{-6} to 3.65×10^{-4} ft/s) were measured using the point dilution test technique. The problems identified with this technique included homogeneous mixing of the tracer in the well, possible density gradients forming with the introduction of the tracer, and changes in the rate at which the tracer moves out of the well due to the well-mixing mechanism. This technique also required the use of a peristaltic pump to draw water from the test section in the well in a closed loop, which in turn required a power source for the pump and the aboveground support equipment.

Several researchers have used nuclear isotope tracers to estimate groundwater flow velocity. Ochiai (1964) performed an early investigation of the use of radioisotopes to measure groundwater flow. Hamada (1999) used the ratio of ^{222}Rn concentration in water before and after it flowed into a well to estimate horizontal groundwater velocity. This method required groundwater residence time in the well being sampled of several days. Hamada reported that the use of ^{222}Rn concentration was applicable to groundwater velocities in the range 10^{-5} to 10^{-6} cm/s (3.28×10^{-7} to 3.28×10^{-8} ft/s). Bardhan (1975) used H_3BO_3 salt, a strong neutron-absorbent tracer, with gamma-gamma and neutron-neutron depth gauges to estimate the vertical groundwater flow in a borehole. This method was sensitive to horizontally induced flow errors due to porous zones in the measurement section. Tests conducted by Bardhan in Poona, India using this method showed laminar, vertical flow with the only turbulence introduced by horizontal flow.

The vertical flow velocity measured by Bardhan was 0.145 cm/sec (4.76×10^{-3} ft/s). Halevy et al. (1967), Drost et al. (1968), and Grisak et al. (1977) have used the dilution of radioisotope tracers with time in boreholes to estimate groundwater velocity. The primary disadvantages of these methods are either the use of expensive and sensitive nuclear-based sondes or the procurement, transportation, and storing of expensive radioisotopes.

Advantages of Fluorescein Dye Adsorption and Dilution Technique

Unlike the direct and indirect measurement techniques described previously, the technique described in this paper uses fluorescein dye adsorbed onto carbon rods to indicate the direction of groundwater flow and the dilution of fluorescein dye with groundwater in a controlled release mechanism to provide an indication of groundwater flow velocity. This technique has several advantages over the methods previously described including providing groundwater flow direction and velocity measurements in a single well in a relatively short length of time (generally less than 3 hours) using a simple, easy to operate, and inexpensive measurement device. The device cost was under $300 with minimal additional costs associated with procuring fluorescein dye and carbon rods. No packers, pumps, or electrical power is needed to perform the measurements. The amount of fluorescein dye released into the well is small with the majority of the dye returned from the well as part of the sample required for the groundwater flow velocity measurement. The samples returned from the well are easy to store for transport to a laboratory and only require minimal processing prior to measurement with a fluorometer. The detection threshold for the fluorescein dye adsorbed by the carbon rods is only limited by the sensitivity of the fluorometer used to process the samples returned from the well. In the experiments discussed below, the fluorometer was able to detect fluorescein dye at a concentration 0.023% of the original dye concentration released into the groundwater flow.

Measurement Theory

This project proposed to use a dye fluorescence method for determining the magnitude and direction of groundwater flow in a well. It was hypothesized that fluorescein dye introduced into groundwater would be adsorbed onto the surface of carbon rods. Once the carbon rods were removed from the groundwater and dried, the fluorescein dye that was adsorbed onto the carbon could be released by using an organic solvent. The solvent and dye could then be placed in a fluorometer and the relative concentration of fluorescein dye in the solvent detected and measured. Therefore, the greater the intensity of fluorescence in a sample of solvent and fluorescein dye, the greater the amount of dye that flowed past the carbon rod. If this were true, the direction of groundwater flow could be determined by placing carbon rods at several evenly spaced locations around the inside perimeter of a well. The carbon absorption sites downstream from the release point for the fluorescein dye should have the highest concentrations of adsorbed dye thus indicating the direction of flow.

Theoretically, the velocity of groundwater flow could also be measured using fluorescein dye. It was hypothesized that if a container of fluorescein dye were allowed to interact with flowing groundwater through a small hole in the base of the container, the difference in the concentration of fluorescein dye between the inside of the container and the groundwater would result in the exchange of groundwater and dye through diffusion of fluorescein dye into the groundwater. The rate at which the dye diffuses into the groundwater should be a function of the velocity at which the groundwater passes the hole in the container since the concentration of fluorescein dye in the immediate vicinity of the hole will be constantly reduced as the dye is swept away in the flow stream.

Based on these hypotheses, both the groundwater flow direction and velocity measurements could be made using a single dye release container in a single well. This assumption formed the basis for the design of the test set-up and instrument used in the experiments described in this thesis.

Several of the previously identified direct methods measured groundwater velocity as the water moved through the well, which is in fact a man-made cavity inside a porous aquifer material. Drost et al. (1968) recognized that the groundwater flow through a well differs from the true velocity of the groundwater flow in the porous aquifer material. Their equation, as modified by Freeze and Cherry (1979), estimated the groundwater velocity (v) as follows:

$$v = \frac{v^*}{\alpha n} \tag{1}$$

where v^* was the apparent groundwater velocity, α was the groundwater focusing or well-shape factor, and n was the porosity of the porous medium. The groundwater focusing or well-shape factor α depends on the well screen geometry and the hydraulic conductivity of the well pack material (sand or gravel) and was estimated to be in the range 0.5 to 4.0 in sand and gravel aquifers (Drost et al., 1968). According to Freeze and Cherry (1979) the apparent groundwater velocity differs from the true groundwater velocity due to higher hydraulic conductivity in the well as compared to the surrounding porous medium and the effects of porosity in the porous medium and the well screen. For the experiments described in the following sections, the groundwater velocity measured was the apparent velocity, v^*. Because the test apparatus used in the experiments described in this thesis was a closed system with no path for the groundwater to flow around the well, the apparent groundwater velocity was simulated.

Groundwater Flow Simulation

The ideal test for measuring groundwater discharge in a single well using fluorescein dye would involve an actual well; however, control of the groundwater flow rate could not be achieved. A secondary concern associated with an actual well was that observation of the fluorescent dye release and the time it takes for the dye to move out of the well would be difficult if not impossible. Therefore, it was decided to simulate groundwater flow in a laboratory test apparatus developed specifically for this project. The test apparatus, shown in Figures 1 and 2, was constructed of plastic storm water drainage and sanitary sewer

pipes and fittings purchased at local hardware stores. The simulated aquifer consisted of three standpipes linked by pipes near their bases. The standpipes provided pressure head to the system and served as a means to reduce the flow velocity and currents in the system. The cross-link pipes provided the means to provide direction to the flow as well as serving as the location for mounting porous media to simulate the aquifer.

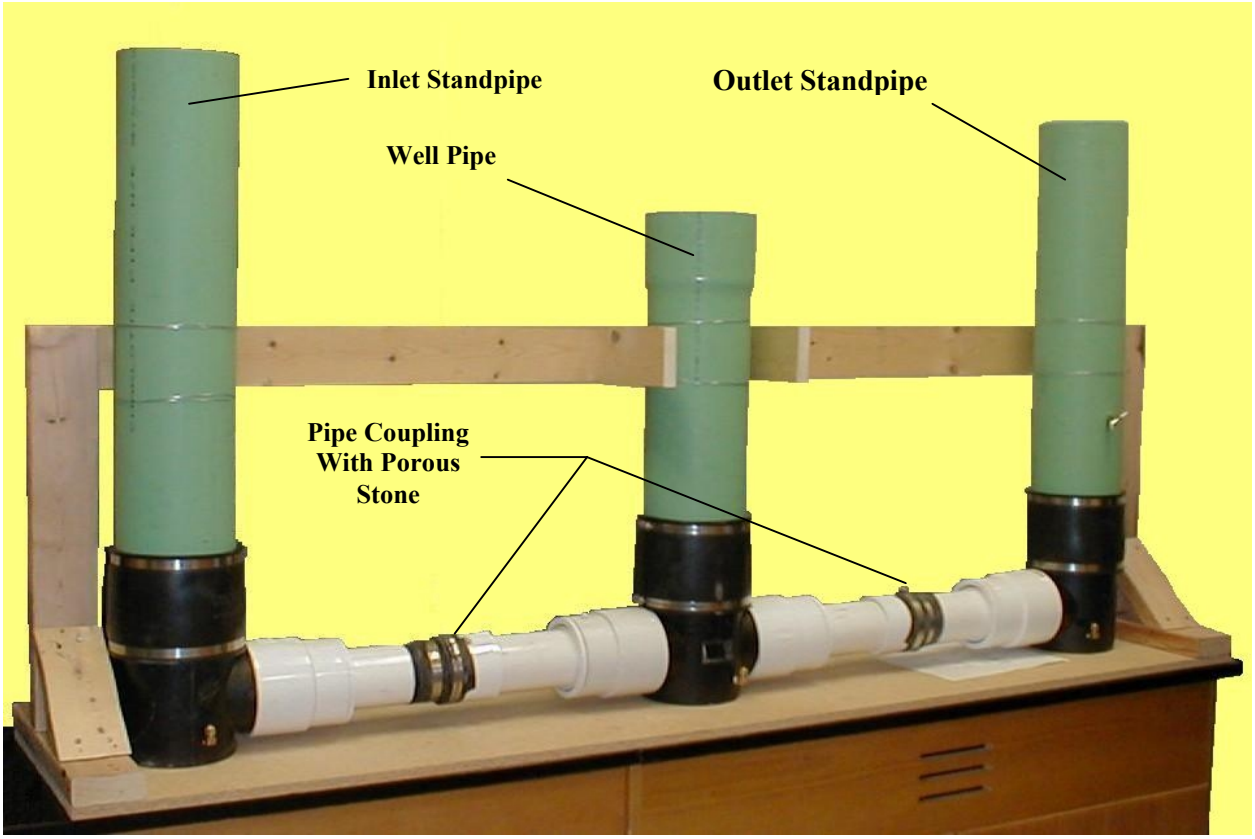

Fig. 1. Test apparatus with manometers removed to show well pipe.

Each standpipe consisted of 152.4 mm (6-inches) diameter polyvinyl chloride (PVC) pipe. The two outer standpipes were both 965.2 mm (38 inches) high, measured from the tabletop datum, and used as the inlet and outlet for the water flowing through the system. The middle pipe was 774.7 mm (30.5 inches) high and served as the simulated well. An elbow fitting with a pipe diameter reducer was used at the bottom of the inlet and outlet standpipe while a T-fitting was used at the bottom of the well standpipe. The inlet and outlet standpipes and the simulated well pipe were sealed to the elbow fittings and T-fitting using 152.4

mm (6 inch) diameter neoprene sleeves with stainless steel slotted pipe bands that were tightened to prevent leakage. A 152.4 mm to 127.0 mm (6 inch to 5 inch) diameter PVC reducing coupling was inserted over and glued to the 152.4 mm (6 inch) diameter horizontal openings in the elbows and T-fitting. A 127.0 mm to 101.6 mm (5 inch to 4 inch) diameter PVC bushing was inserted into and glued to each of the reducing couplings.

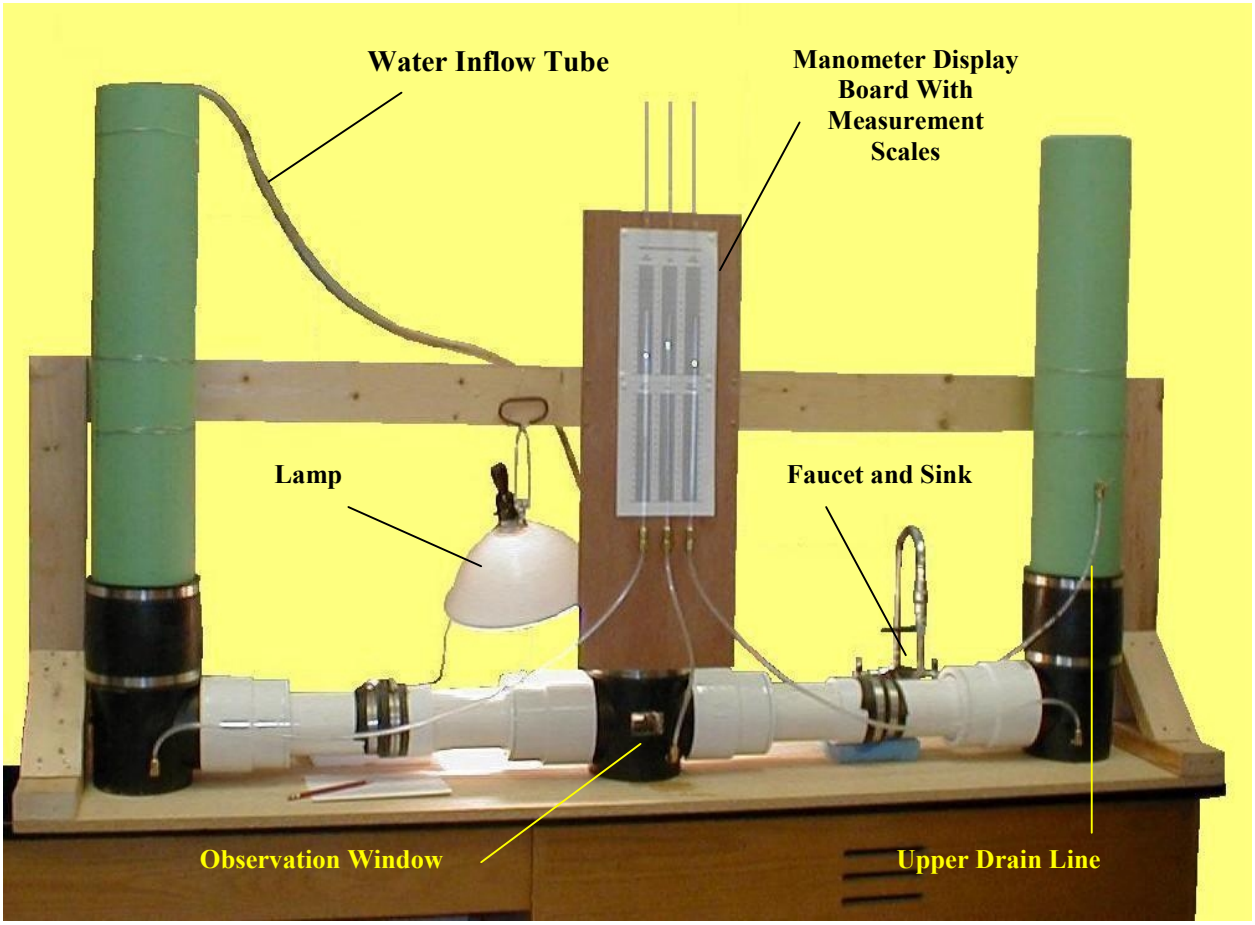

Fig. 2. Test apparatus configured for flow velocity and direction measurement. A second (lower) drain line is located on the backside and near the base of the outlet standpipe. Both drain lines discharge into the sink.

The T-fitting at the base of the simulated well pipe also served as the test chamber for the groundwater flow measurement device. Two window openings were cut into the T-fitting to allow observation of the fluorescein dye release and the movement of the dye. The windows were formed by heat deforming

transparent Plexiglas over a wood form shaped to conform to the inside surface of the T-fitting. The windows were held in place and sealed using a silicon-based sealant.

Each of the standpipes (inlet and outlet) was connected to the well pipe using two sections of 101.6 mm (4 inch) diameter PVC pipe linked with a PVC coupling. The downstream end of the PVC coupling was glued to the PVC pipe while the inlet end was only snug fit to allow disassembly of the test set-up and access to a porous stone inserted in the flow path at the coupling. A porous stone was inserted in the 101.6 mm (4 inch) diameter PVC pipe at the coupling upstream and downstream of the well pipe to simulate unconsolidated aquifer material (sand and gravel). The upstream PVC coupling joint was sealed with a silicone based caulk and the joint was then covered with a stretched rubber strip held in place with stainless steel slotted pipe bands that were tightened to prevent leakage. The free ends of each of the PVC pipe/coupling/porous stone assemblies were inserted and glued into the 127.0 mm to 101.6 mm (5 inch to 4 inch) diameter PVC bushings mentioned previously.

The porous stones were made out of a ceramic formed from fused crystalline aluminum oxide ("Norton stone") as supplied by Durham Geo Enterprises, Stone Mountain, Georgia, with their permeability testing equipment for geotechnical testing laboratories. The porous stone material was reported to have an average pore size of 179 microns and a permeability coefficient in the range 71.85 to 86.22 darcies (7.09 x 10^{-7} to 8.51 x 10^{-7} cm^2). The permeability coefficient for the porous stones compared favorably with permeability coefficients in the range 10^{-2} to 10^{5} darcies (10^{-10} to 10^{-3} cm^2) reported for silty sand to gravel (Freeze and Cherry, 1979). The porous stones were 71.12 mm (2.8 inches) in diameter and 6.35 mm (0.25 inches) thick. An adapter ring was machined out of 9.53 mm (0.375 inch) thick polyethylene material to hold each of the porous stones in place. The adapter ring fit snugly inside the PVC coupling.

Construction of the adapter ring/porous stone assembly consisted of the following steps: 1) a bead of silicone caulk was placed along the seating edge of the adapter, 2) the porous stone was placed into the

adapter against the silicone caulk and seating edge, 3) another bead of silicone caulk was placed in the gap between the inner surface of the adapter ring and the outer edge of the porous stone, and 4) a Plexiglas ring was placed over the porous stone and adapter and held in place with four brass screws. The various parts used in this assembly are shown in Figure 3. The adapter ring and Plexiglas cover ring reduced the effective diameter of the porous stone to 63.5 mm (2.5 inches). The completed adapter ring/porous stone assembly was then inserted into the PVC coupling against the pipe stop inside the coupling and silicone caulk placed around the outer circumference of the adapter ring, Figure 4. The use of silicone caulk along the edges of the porous stone and adapter ring was to prevent water from leaking around the edges of the porous stone.

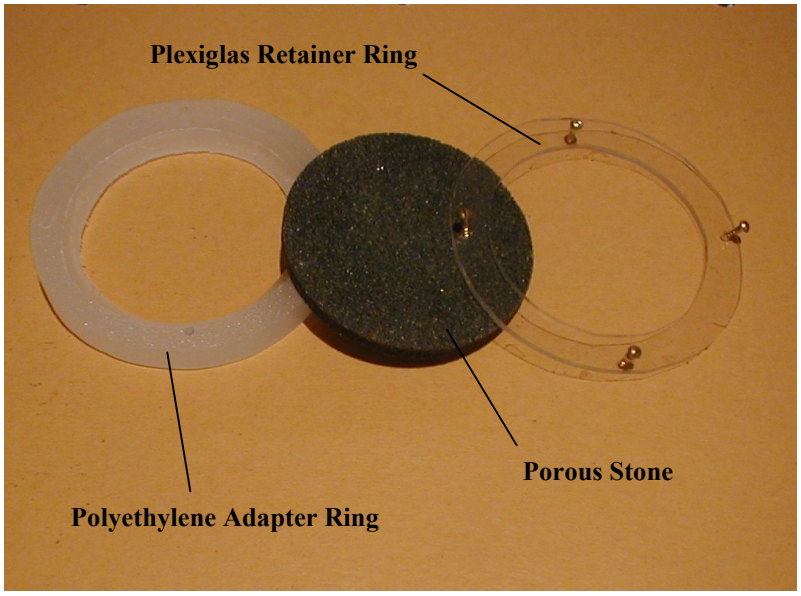

Fig. 3. Porous stone and adapter ring assembly.

Fig. 4. Porous stone/adapter ring assembly installed in PVC

A 19.05 mm to 6.35 mm (0.75 inch to 0.25 inch) brass elbow fitting with compression coupling was tapped into each of the PVC elbow fittings near the base of the inlet and outlet standpipes and near the base of the PVC T-fitting at the base of the simulated well pipe. The compression tube couplings were used to connect flexible 6.35 mm (0.25 inch) diameter clear vinyl manometer tubes. The flexible manometer tubes for the inlet standpipe, simulated well, and outlet standpipe were extended to the center of the test set-up and connected to rigid, clear plastic tubes using brass compression couplings that were mounted on a display board located in front of the simulated well pipe and above the observation windows. A scale graduated in millimeters was placed behind the rigid manometer tubes to provide the means to determine the head in each of the standpipes and well pipe relative to each other. The manometer tubes and their measurement scales are shown in Figure 5.

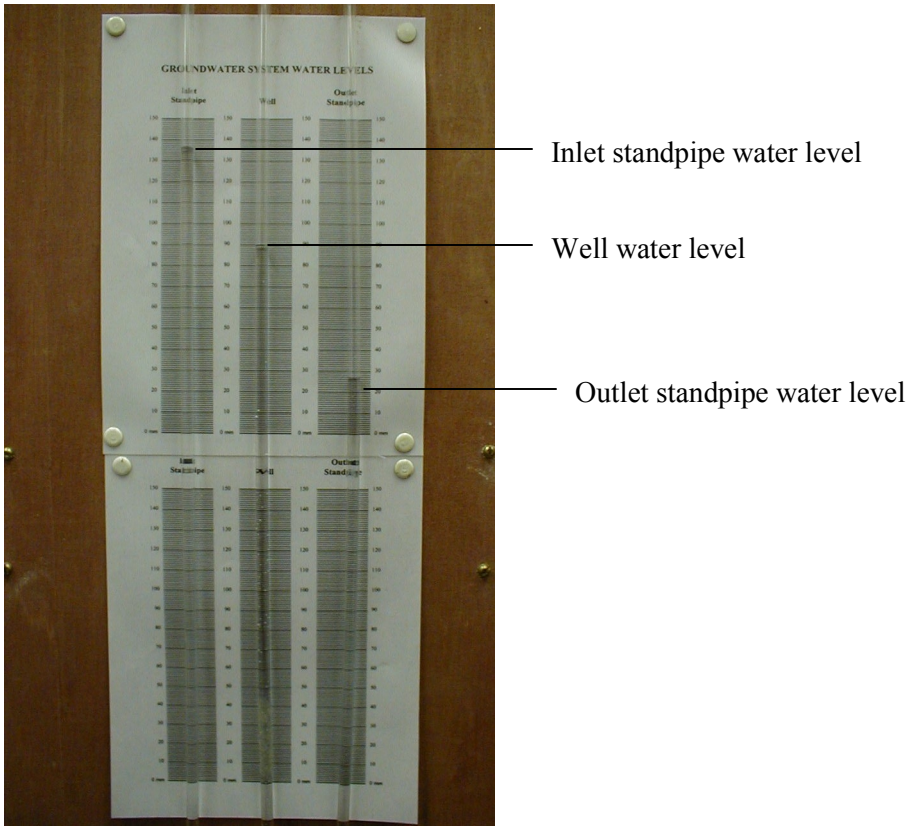

Fig. 5. Manometer display board showing differential water levels in the manometers during a groundwater flow experiment.

Two 19.05 mm to 6.35 mm (0.75 inch to 0.25 inch) brass gate valves with compression couplings were tapped into the rear of the outlet standpipe, one near the base of the pipe and the other about half-way up the pipe's height. These valves provided the means to control the outflow from the test apparatus and to drain the test apparatus when the experiments were over. Flexible 6.35 mm (0.25 inch) diameter clear vinyl tubing was connected to each valve and extended to a sink next to the test set-up.

The entire test apparatus was mounted on a wood frame to prevent accidental movement of the various components.

Measurement Device

The groundwater flow magnitude and direction measurement device used for this project is illustrated in Figure 6 with the various parts of the instrument that are identified in the following paragraphs labeled on the figure. The primary components of measurement device were two polyethylene disks that formed the upper and lower boundary of the measurement section in the well. The disks were both 149.23 mm (5.875 inches) diameter by 9.53 mm (0.375 inch) thick to allow easy insertion and travel down the well pipe.

The upper (moveable) polyethylene disk was attached to the bottom of a 9.53 mm (0.375 inch) diameter by 0.914 m (3.0-foot) aluminum slide rod. A thread was cut into the lower approximately 25.4 mm (1.0 inch) of the aluminum slide rod, and the polyethylene disk was secured to the aluminum slide rod using two 12.70 mm (0.5 inch) nuts and washers.

A slide cage formed from four 3.18 mm (0.125 inch) diameter by 254 mm (10.0 inch) long brass rods onto which threads were cut for a short length on each end. The brass cage rods were bent into 90º angles with the longer leg measuring 190.5 mm (7.50 inches). A brass nut (not shown in Figure 6) was threaded onto the upper end (short leg) of each of the brass slide cage rods and then the brass slide cage

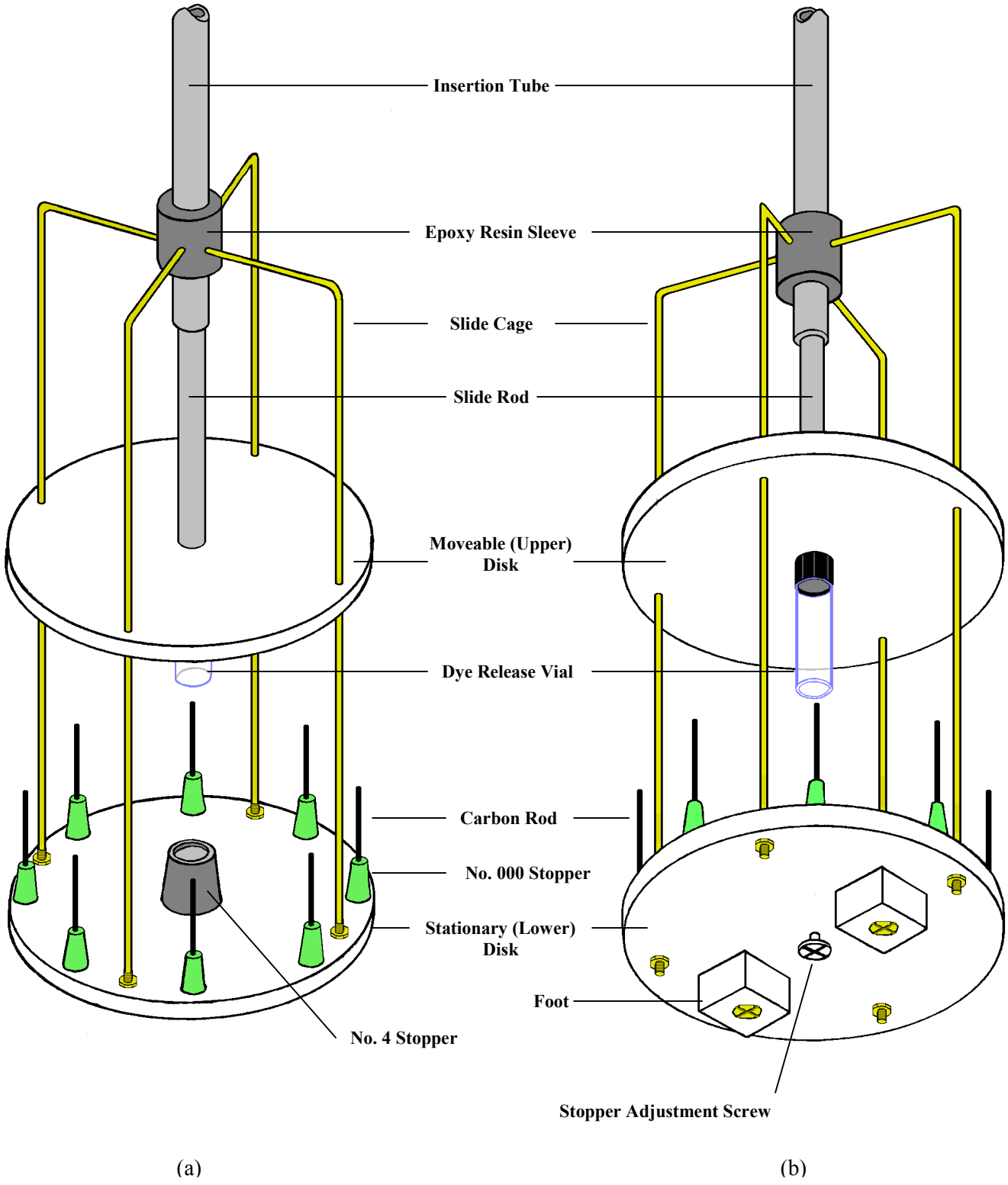

Fig. 6. Illustration of the groundwater flow direction and velocity measurement device with oblique views looking (a) down and (b) up.

rods were screwed into an epoxy resin sleeve bonded to a 12.75 mm (0.5 inch) diameter aluminum insertion tube. The purpose of the nuts was to provide positive tension on the connection between the brass slide cage rods and the insertion tube.

The epoxy sleeve was constructed by first applying masking tape in layers around the circumference of the insertion tube at the upper and lower limit of the desired length of the sleeve and to the desired thickness of the sleeve. Then epoxy resin was painted onto the tube in successive coats and cured until the desired thickness was achieved. The epoxy was then sanded to achieve a uniform thickness. The purpose of the epoxy resin sleeve was to provide additional thread length for the brass rod connection to the insertion tube.

Once the short ends of the brass slide cage rods were attached to the aluminum insertion tube, they were passed through holes of a slightly larger diameter in the upper (moveable disk). Then the bottom end of each brass rod was secured to the lower disk using a pair of washers and brass nuts. The upper (moveable) disk was free to slide vertically along the brass rod slide cage.

The aluminum slide rod attached to the upper (moveable) disk was inserted into the aluminum insertion tube and was free to slide within the tube. Thus, the upper polyethylene disk was free to move vertically with respect to the stationary lower polyethylene disk.

The dye release mechanism for the device consisted of a glass vial containing fluorescein dye with a salt plug to prevent introduction of the dye into the groundwater flow until turbulence caused by the introduction of the groundwater flow magnitude and direction measurement device dissipated to the point that laminar flow once again dominated in the test section of the simulated well. Based on Kearl's (1997) investigations, it was considered that the salt plug had to take at least 30 minutes to dissolve before the fluorescein dye could be released into the simulated well to ensure that laminar flow conditions were

restored to the point that turbulence would not significantly affect the experiment results. The glass vial used in the experiments was a standard 17 mm diameter by 60 mm long (0.657 inch diameter by 2.360 inch long) screw-cap vial attached to the upper (moveable) polyethylene disk using a brass screw drilled through the cap of the vial into a threaded hole tapped into the base of the aluminum slide rod. The bottom of the glass vial was removed by cutting with a diamond-faced grinding bit. While the instrument was being lowered into the well, the bottom of the glass vial was protected from exposure to water by imbedding it into a shallow hole countersunk into the top of a No. 4 rubber stopper. The No. 4 rubber stopper was secured to the lower (stationary) polyethylene disk using a nylon screw inserted through a hole in the disk and into a hole drilled into the back of the rubber stopper. When the upper (moveable) polyethylene disk was raised using the aluminum slide rod, the open end of the glass vial was pulled from the rubber stopper exposing the salt plug to water.

Carbon rods were used to capture the dye released in this experiment. The carbon rods each measured 3.05 mm (0.12 inch) in diameter by 40 mm (1.57 inches) long and were positioned at eight evenly spaced locations along the circumference of the lower (stationary) polyethylene disk and 6.35 mm (0.25 inch) from the edge of the disk. Each carbon rod location was numbered in a clockwise manner (looking down on the top of the disk) and the numbers engraved into the disk. Initially, the carbon rods were inserted in holes drilled into No. 000 rubber stoppers that were inset into shallow holes drilled into the lower (stationary) polyethylene disk. Later in the sequence of experiments, for reasons discussed below, the rubber stoppers were eliminated and the carbon rods were inserted into modeling clay pressed into the shallow holes in the lower (stationary) polyethylene disk.

Additional features of the groundwater flow magnitude and direction measurement device include two square polyethylene feet, each 25.4 mm (1.0 inch) square by 19.05 mm (0.75 inches) thick screwed into the bottom of the lower (stationary) polyethylene disk using brass screws. The feet elevated the lower disk off the bottom of the well pipe to a point where the top of the lower disk was level with the

horizontal flow area in the well pipe. If the feet were not used, eddies would likely form as the simulated horizontal groundwater flow expanded into the vertical well pipe and then contracted to exit the well pipe.

Lastly, a flat-head thumbscrew was tapped into the aluminum insertion tube near the top of the tube to secure the aluminum slide rod in the up position during the experiments.

Dye Release Vial Preparation

Prior to the beginning of a series of experiments, several of the dye release vials were prepared. The salt plugs were first cut out of a salt block using a plug-cutter drill bit inserted into a drill motor. Because of the vibration created between the drill bit and the salt block during the drilling and the brittleness of the salt, the salt plugs tended to break inside the drill bit after attaining an average thickness of about 3.8 mm (0.15 inch). Therefore, it was initially decided to use two salt plugs stacked vertically to delay the entry of fluorescein dye into the simulated well.

Several materials were tried to provide a seal between the open end of the glass vial and the salt plugs including silicone caulk, rubber cement, and a brine solution to which salt was continuously added while heating to create supersaturated conditions with the intent of creating a crystalline matrix that would adhere to both the glass and salt plugs when cooled. However, it was found that although these materials generally adhered to the glass, they either would not seal against the salt plug surface or dissolved too rapidly to effectively delay the flow of fluorescein dye into the simulated well.

Eventually, oil-based modeling clay was found to provide a seal against the inside walls of the glass vial and the salt plugs. A small portion of modeling clay was rolled out into a thin layer and the salt plugs were stacked on top. Next, another portion of modeling clay was rolled into a thread and pressed around the perimeter of the salt plugs and melded into the exposed surface of the bottom layer of modeling clay. The end of a 2.92 mm (0.115 inch) diameter wooden dowel was placed atop the center of the upper salt

plug and additional modeling clay was pressed into place between the dowel and the modeling clay surrounding the outer perimeter of the salt plugs. This left a small hole in the modeling clay exposing the top of the upper salt plug. The open end of the glass vial was then pushed over the modeling clay/salt plug assembly. The wooden dowel was inserted through the top (screw end) of the glass vial and used to tamp the modeling clay around the inner surface of the glass vial to improve the seal between the modeling clay and the glass. The glass vial with the modeling clay/salt plug inserted in the end was inverted and the wooden dowel was used to form a 2.92 mm (0.115 inch) diameter hole in the bottom of the modeling clay exposing the bottom surface of the lower salt plug. A cone shape depression was formed in the modeling clay with the hole at its center to encourage any trapped air bubbles to concentrate at the hole. The salt plug assembly is illustrated in Figures 7 and 8.

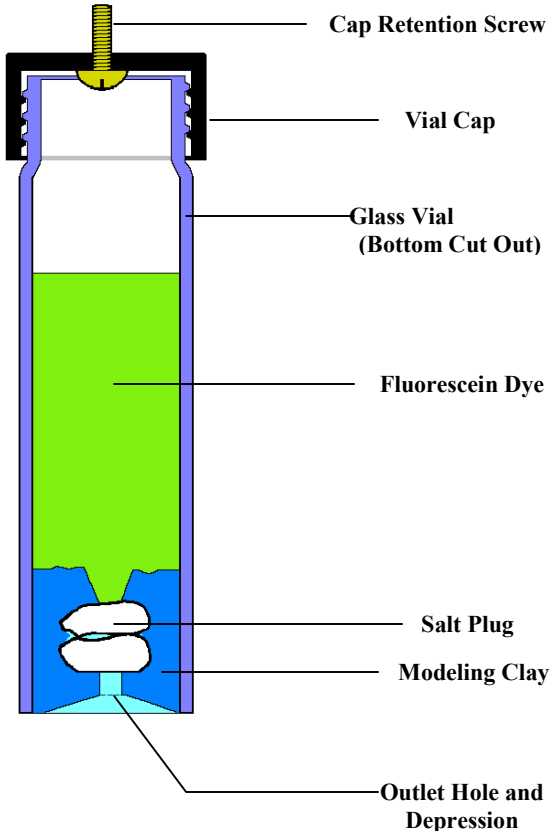

Fig. 7. Cut-away illustration of the dye release vial.

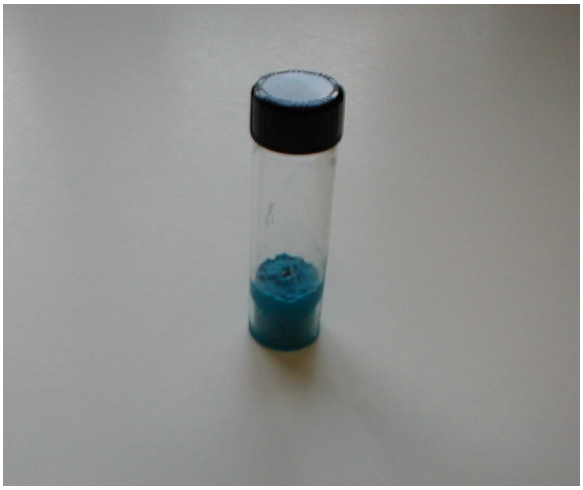

Fig. 8. Dye release vial with modeling clay/salt plug in place. Note hole in top of modeling clay.

Experiment Procedure

Before any of the experiments were begun, the fluorescein dye was prepared by mixing 37.6 mg of fluorescein disodium salt ($C_{20}H_{10}O_5Na_2$) with 100 ml of water to produce a 1.0 molar solution. The 1.0 molar solution was used throughout the series of experiments.

An experiment with the groundwater flow direction and velocity measurement device began by filling the test apparatus with water. The valves in the outlet standpipe were closed and a water tube from a sink adjacent to the test apparatus was used to fill the inlet and outlet standpipes and the simulated well pipe. The water was then shut off and the water levels were allowed to stabilize as shown by equal levels within the piezometers for the inlet and outlet standpipes and the simulated well pipe.

Once the test apparatus was filled and it was verified that there were no significant leaks, the lower valve in the outlet standpipe was slowly opened and water was trickled into the inlet standpipe through the water tube from the adjacent sink. During the course of an experiment, it was attempted to keep the water level in the simulated well pipe as high as possible without causing water to overflow either the inlet standpipe or the simulated well pipe. Once the outlet valve was open, a hydraulic gradient began to form immediately between the inlet standpipe, simulated well pipe, and the outlet standpipe. Varying the inflow rate and/or adjusting the outlet valve opening established a balance between the amount of water entering and exiting the test apparatus. Once the water levels shown by the piezometers became steady, the flow rate was measured. This was accomplished by capturing water flowing from the discharge valve in the outlet pipe in a graduated cylinder over a measured period of time. The flow rate was measured several times throughout an experiment to verify that the flow was remaining constant.

Next the groundwater flow direction and velocity measurement device was prepared. Eight 3.05 mm (0.12 inch) diameter by 40 mm (1.57 inches) long carbon rods were inserted into the holes in the tops of the No. 000 rubber stoppers around the perimeter of the lower (stationary) polyethylene disk.

Throughout all of the experiments, the carbon rods were handled with latex gloves to prevent any contaminants from adsorbing onto the carbon surface. One of the glass vials prepared with the modeling clay/salt plug inserted in the cut end was filled with 5 ml of fluorescein dye and immediately screwed into the cap attached to the upper (moveable) polyethylene disk. The device was then immediately inverted to stop the fluorescein dye from dissolving the salt plug before the groundwater flow direction and velocity measurement device was lowered into the simulated well. The upper (moveable) polyethylene disk was pushed towards the bottom (stationary) polyethylene disk until the bottom of the glass vial was covered by the depression in the top of the No. 4 rubber stopper. The device was kept in an inverted position until the test apparatus was checked again to ensure that the flow conditions were constant. Figure 9(a) shows the device with the glass vial filled with fluorescein dye and the bottom of the glass vial embedded in the No. 4 rubber stopper.

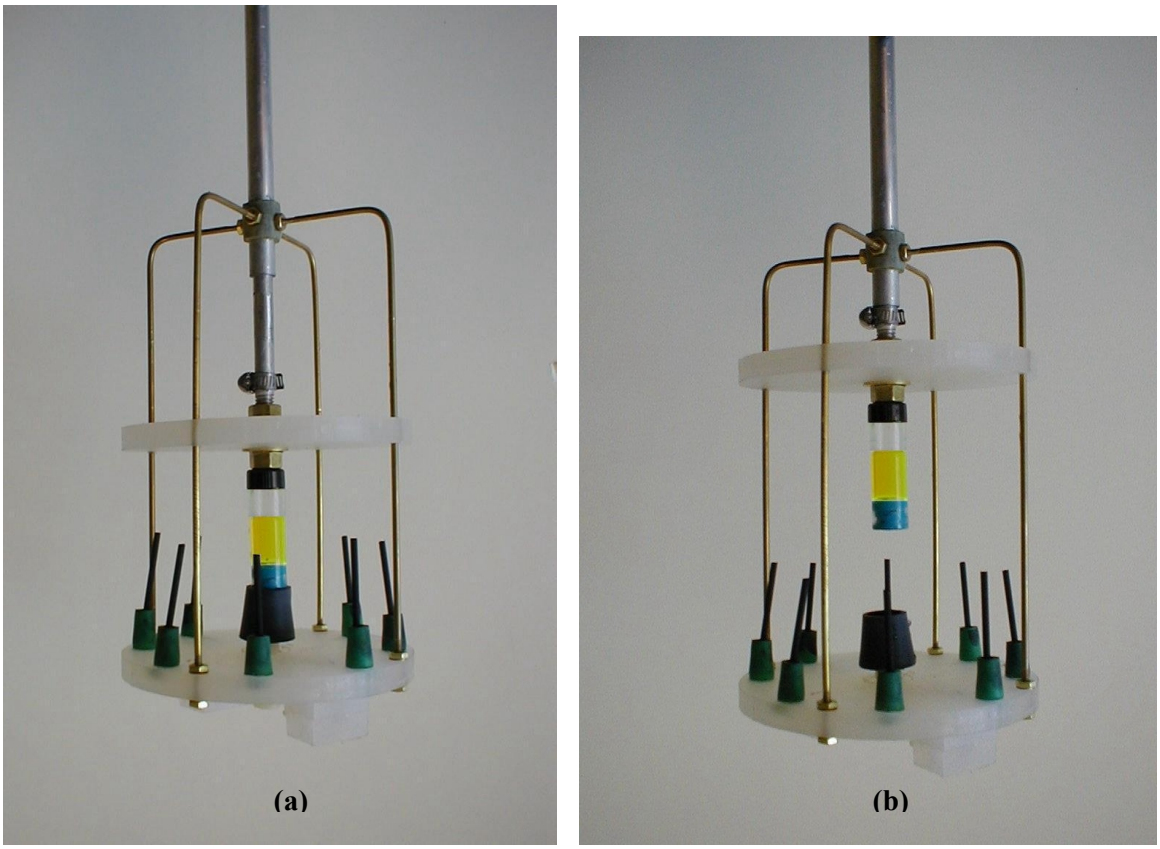

Fig. 9. Groundwater flow direction and velocity measurement device (a) prepared for insertion in the simulated well with the bottom of the dye release vial and salt plug protected by a No. 4 rubber stopper, and (b) with dye release vial in position to expose salt plug to water.

The groundwater flow direction and velocity measurement device was then returned to its upright position and inserted into the simulated well pipe in the test apparatus until the feet on the bottom of the lower (stationary) polyethylene disk made contact with the bottom of the simulated well pipe. The lower (stationary) polyethylene disk was held in place using the insertion tube while the upper (moveable) polyethylene disk was raised using the slide rod. A cap screw near the top of the insertion tube was used to hold the slide rod and hence the upper (moveable) polyethylene disk in the raised position for the duration of the experiment. Raising the upper (moveable) polyethylene disk exposed the bottom of the glass vial with the salt plug to the water in the simulated well. Figure 9(b) shows the device outside of the simulated well with the upper and lower polyethylene disks separated and the glass vial and salt plug in the position to be exposed to water. The salt plug then slowly dissolved over a period that averaged 105 minutes as the simulated groundwater flow passed the hole in the bottom of the modeling clay/salt plug. Once the salt plug dissolved, fluorescein dye exchanged with the water and flowed from the dye release vial.

The fluorescein dye was entrained by the water in the direction of the groundwater flow and passed the carbon rods inserted within the flow stream. Some of the fluorescein dye was adsorbed onto the surface of the carbon rods while the remainder passed through the outlet side of the test apparatus.

Once the fluorescein dye was allowed to flow into the simulated well for a length of time that was varied for each experiment, the thumb screw on the insertion tube was loosened, and the slide rod connected to the upper (moveable) polyethylene disk was pushed down covering the end of the dye release vial in the depression on top of the No. 4 rubber stopper. This stopped the flow of fluorescein dye into the simulated well. The groundwater flow direction and velocity measurement device was then slowly withdrawn from the simulated well and immediately inverted to prevent the accidental escape of any more fluorescein dye. The carbon rods were removed from the lower (stationary) polyethylene disk and stored in glass test tubes labeled with the experiment number and numbers corresponding to the rod positions on the lower

(stationary) polyethylene disk. The carbon rods were allowed to dry for a minimum of seven days. At the end of the drying period, the carbon rods were inserted into plastic screw top vials and soaked in 5.0 ml of methanol (CH_3OH) for a minimum of seven days to release the adsorbed fluorescein dye from the surface of the carbon.

While in the inverted position, the upper (moveable) and lower (stationary) polyethylene disks were once more slid apart exposing the now depleted salt plug. A plastic screw top vial was positioned over the end of the dye release vial and held in place while the groundwater flow direction and velocity measurement device was returned to its upright position. The dye release vial was slowly unscrewed from the cap attached to the upper (moveable) disk which allowed air pressure inside and outside of the vial to equalize immediately releasing the fluorescein dye/water mixture in the dye release vial to flow through the hole in the modeling clay at the bottom of dye release vial into the plastic screw top vial. A lid was immediately screwed onto the plastic vial that was labeled with the experiment number.

If another experiment was to be run on that day, the groundwater flow direction and velocity measurement device was prepared for the next experiment with a new set of carbon rods and another prepared dye release vial. Otherwise, the water from the sink flowing into the inlet standpipe was shut off, and the upper and lower drain valves on the outlet standpipe were opened to drain the test apparatus.

Observations

Once the dye release vial attached to the groundwater flow direction and velocity measurement device was raised out of the No. 4 rubber stopper, an air bubble usually lodged against the exposed salt plug. While the air bubble did not significantly affect the experiment, it did serve to lengthen the time before fluorescein dye was released from the dye release vial. Attempts to change the end configuration of the modeling clay around the hole exposing the salt plug did not significantly reduce the size or position of

the air bubble. The water film on the salt plug began to dissolve the salt plug; however, and the air bubble eventually passed through the salt plug.

After the air bubble cleared the bottom of the salt plug and rose to the top of the fluorescein dye inside the glass vial, full contact between the salt plug and the water in the simulated well occurred. At this point, a density current of dissolved salt and water began to flow from the hole in the modeling clay. This density current was easily observed through the window in the test apparatus and appeared as a translucent, clear thread that flowed straight down into the depression in the No. 4 rubber stopper. The density current likely caused eddy currents to form in the test section prior to the release of fluorescein dye. Figure 10 is a photograph of the salt density current taken through the front observation window of the test apparatus. Observations of the salt density current and the fluorescein dye were aided by shining light from the lamp mounted on the test apparatus on a white sheet placed behind the rear window of the test apparatus.

The salt-water flow eventually filled the depression in the No. 4 rubber stopper and began to overflow on all sides of the stopper. The salt density current did not appear to integrate with the groundwater flow until after it hit the bottom of the test section. This indicates that there was insufficient mixing length between the bottom of the dye release vial and the bottom of the test section over which the differences in density and temperature between the groundwater and the salt water could generate sufficient turbulence to cause mixing. On average the salt plug took approximately 105 minutes to dissolve, which exceeded the 20 to 30 minutes reported by Kearl (1997) for any turbulence caused by the insertion of the groundwater flow direction and velocity measurement device into the simulated well to be dominated by laminar flow. In most cases, dye was not observed to flow until the entire salt plug had dissolved. This may be due to the concentrated salt water accumulated at the exit hole in the modeling clay having a higher density than the fluorescein dye. Several of the remaining modeling clay portions of the modeling clay/salt plugs were dissected following their use which confirmed that all of the salt had dissolved.

Fig. 10. View through the groundwater flow direction and velocity measurement device window showing the salt density current before the start of the fluorescein dye release.

In most, but not all, cases the fluorescein dye began to flow immediately after the salt plug had dissolved. The dye flowed in a thin thread from the bottom of the dye release vial through the hole in the modeling clay. At first, the fluorescein dye flowed straight down into the depression in the top of the No. 4 rubber stopper. This was attributed to the dye having a relatively greater density. However, as the water and fluorescein dye exchanged across the boundary at the bottom of the hole in the modeling clay, the density of the fluorescein dye decreased and the dye thread began to bend with the direction of the groundwater flow in the simulated well. Figure 11 is a photograph of the dye taken through the front observation window in the test apparatus. It was also observed that the fluorescein dye accumulated at the downstream end of the lower (stationary) polyethylene disk in a crescent-shaped wedge with the thickest portion of the wedge aligned with the center of the flow section in the test apparatus. Because of the

accumulation of the dye atop the lower (stationary) polyethylene disk, it was decided for several experiments to eliminate the No. 000 rubber stopper holding the carbon rods and instead embed the carbon rods directly into modeling clay inserted into the inset holes in the lower (stationary) polyethylene disk used to hold the rubber stoppers. It was considered that the rubber stoppers might be holding the carbon rods too high to be fully exposed to the fluorescein dye, which appeared to be flowing in a density current along the top of the lower (stationary) polyethylene disk. The results of the experiments did not reveal any advantage in mounting the carbon rods in modeling clay versus the No. 000 rubber stoppers.

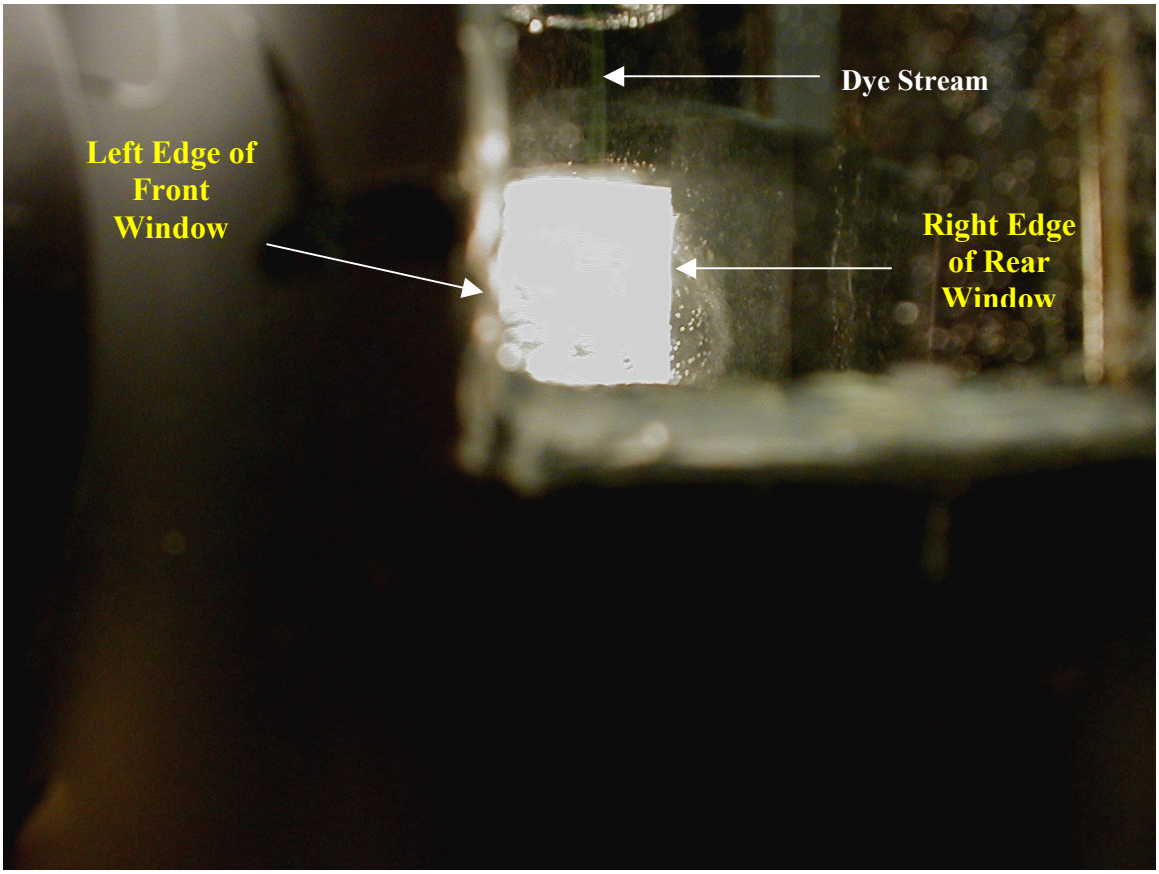

Fig. 11. Angled view through the front window of the test apparatus showing the fluorescein dye stream. The view is angled to provide contrast to reveal the dye stream in the photograph.

The characteristics of the fluorescein dye thread flowing from the bottom of the dye release vial were also observed. During the experiments with the lower water velocities in the test apparatus, the end of the fluorescein dye thread was observed to have a progression of formations starting with the thickening of

the thread into a globule. The globule then attained a cup shape as the upper portion of the globule began to collapse into the center of the globule. The cup shape then flattened into a donut shaped ring that was absorbed into the accumulated dye atop the lower (stationary) polyethylene disk. This progression of dye formations is illustrated in Figure 12. The progression of shapes in the fluorescein dye thread can be attributed to frictional resistance at the boundary layer of the thread. At no time did the fluorescein dye simply dissolve into the water, but rather remained as a coherent thread or the progression of three-dimensional shapes described above. The formation and characteristics of the fluorescein dye thread further confirms the assumption of laminar flow in the simulated well. If the simulated groundwater flow

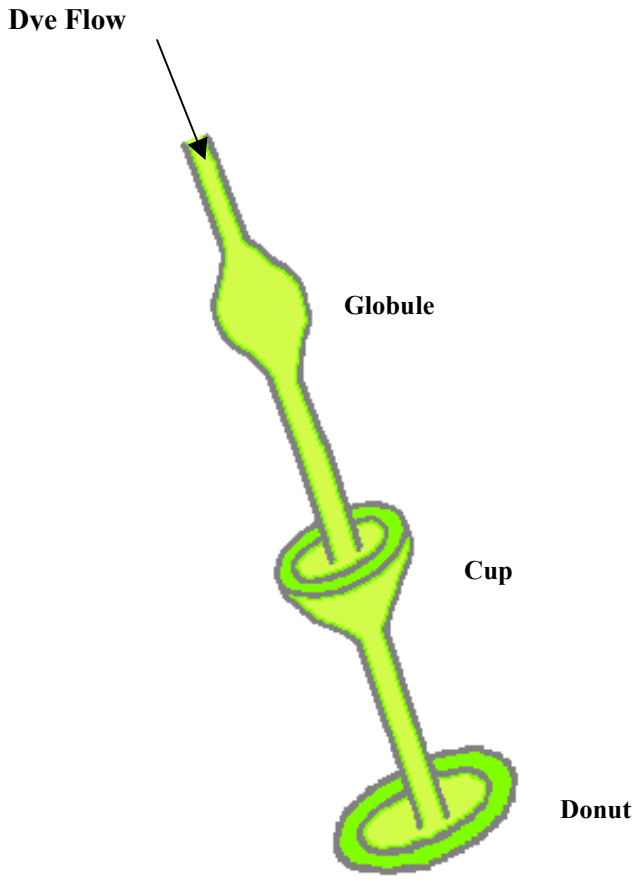

Fig. 12. Sketch of fluorescein dye stream illustrating the progressive formation of globule, cup, and donut-shaped features as the dye thread disintegrates.

had been turbulent, the fluorescein dye thread would have broken apart or otherwise would have more rapidly mixed with the groundwater flow instead of staying in coherent thread-like form with a progression of shapes caused by frictional resistance on the thread boundary layer.

Results

All of the samples obtained during the experiments, including the carbon rods soaked in methanol and the fluorescein dye/water solution remaining in the dye release vials, was analyzed using a Turner Designs fluorometer located at the U.S. Geological Survey water quality laboratory in Columbus, Ohio. Before each sample was analyzed, the fluorometer was zeroed using deionized distilled water. A reference standard consisting of a 1.0 molar solution of fluorescein dye was analyzed at the beginning and end of the experiment sample evaluations to verify the accuracy of the fluorometer.

Groundwater Flow Direction Results. A total of 12 experiments were run in the test apparatus. The first six experiments had the carbon rods installed in the groundwater flow direction and velocity measurement device to determine flow direction. The methanol used to release the adsorbed fluorescein dye from the carbon rods was analyzed in the fluorometer. The fluorometer measurements for the flow direction experiments are presented in Table 1. The time, t, that the carbon rods were exposed to the fluorescein dye flow is shown in Table 1 as well as the measured flow, Q, in the test apparatus. Test No. 1 was performed with static (no flow) conditions in the test apparatus. The bearings shown in Table 1 are relative to assumed compass headings where north is at the downstream end and parallel to the centerline axis of flow in the test apparatus. The numerical values shown in the columns labeled "Rod" are the position number of the carbon rod at each bearing. The position of the 0º carbon rod was varied with each experiment to ensure that the dye flow was not favoring a particular path within the groundwater flow direction and velocity measurement device.

TABLE 1

GROUNDWATER FLOW DIRECTION ANALYSIS
CARBON ROD FLOUOROMETER RESULTS

Bearing (°)	Test No.											
	1		2		3		4		5		6	
	Q =0.00 ml/s t = 35 min.		Q =3.37 ml/s t = 60 min.		Q =2.90 ml/s t = 90 min.		Q =2.17 ml/s t = 30 min.		Q =3.17 ml/s t = 105 min.		Q =2.67 ml/s t = 20 min.	
	Rod	Reading	Rod	Reading	Rod	Reading	Rod	Reading	Rod	Reading	Rod	Reading
0	7	0.030	7	0.020	3	0.040	6	0.060	3	0.055	1	0.030
45	8	0.015	8	0.010	4	0.020	7	0.040	4	0.045	2	0.020
90	1	0.020	1	0.015	5	0.010	8	0.020	5	0.030	3	0.030
135	2	0.030	2	0.010	6	0.010	1	0.025	6	0.025	4	0.015
180	3	0.030	3	0.020	7	0.015	2	0.025	7	0.030	5	0.010
225	4	0.020	4	0.020	8	0.015	3	0.035	8	0.030	6	0.020
270	5	0.030	5	0.025	1	0.015	4	0.030	1	0.035	7	0.015
315	6	0.020	6	0.015	2	0.015	5	0.020	2	0.045	8	0.025

The Table 1 results were normalized based on the maximum fluorometer reading for each experiment and flow rose diagrams were constructed, Figure 13. As expected, there is no dominant direction of flow indicated by the fluorescein dye adsorbed and released from the carbon rods for Test No. 1 because static flow conditions existed for this experiment. Test No. 2 also yielded no particular strong sense of flow direction although observations through the windows in the test apparatus showed fluorescein dye accumulating at the downstream side of the lower (stationary) polyethylene disk. A possible explanation was that the groundwater flow direction and velocity measurement device was withdrawn too slowly from the simulated well at the completion of the experiment, and the carbon rods became contaminated with fluorescein dye that had accumulated on the lower (stationary) polyethylene disk. In subsequent experiments, the groundwater flow direction and velocity measurement device was withdrawn more rapidly from the simulated well.

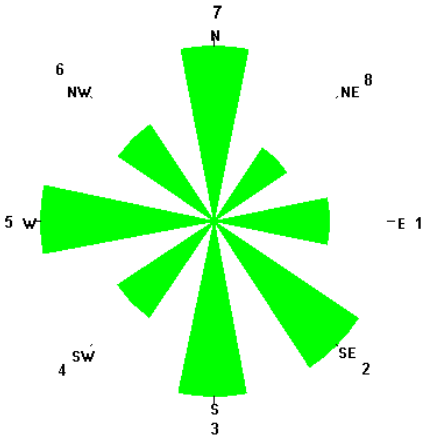

Test 1. Discharge = 0 ml/s; Duration = 35 min.

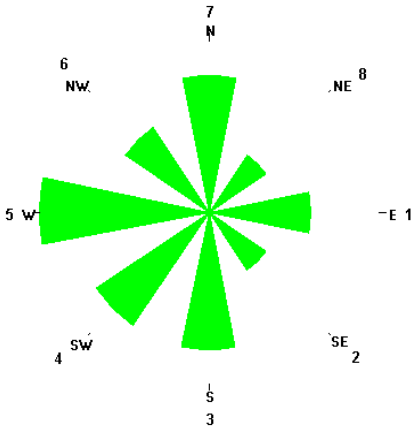

Test 2. Discharge = 3.37 ml/s;

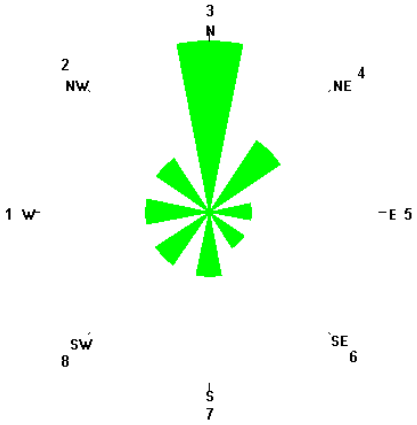

Test 3. Discharge = 2.90 ml/s;

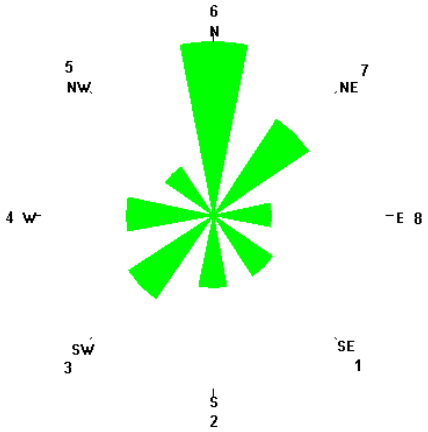

Test 4. Discharge = 2.17 ml/s;

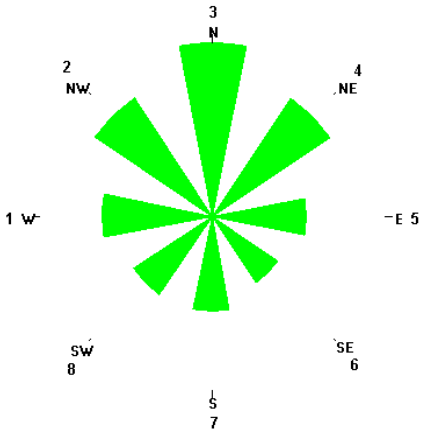

Test 5. Discharge = 3.17 ml/s;

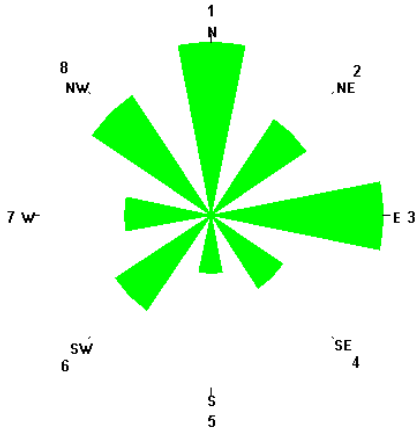

Test 6. Discharge = 2.67 ml/s;

Fig. 13. Flow direction roses normalized to the individual test maximum flow. Flow was introduced into the test chamber from the south and exited to the north. The numbers next to the compass points refer to the carbon rod positions on the test device.

Test Nos. 3 through 6 yielded more promising indications of groundwater flow direction. The variation in the time that fluorescein dye was permitted to contact the carbon rods in each experiment did not appear to affect the amount of fluorescein dye adsorbed onto the carbon rods. The highest fluorometer readings for Test No. 4 and Test No. 5 listed in Table 1 show that a higher concentration of fluorescein dye was adsorbed by the 0º bearing carbon rod in Test No. 4 even though the experiment time was 75 minutes less than Test No. 5. This result could be attributed to the variability in the adsorption characteristics of the carbon rods or a thicker layer of fluorescein dye accumulated atop the lower (stationary) polyethylene disk at slower groundwater flow velocities. Test No. 6 shows a dominant flow direction towards the 0º bearing carbon rod, but also towards the 90º bearing carbon rod. Test No. 6 had a short time duration (20 minutes) and low fluorometer readings, which suggests that the carbon rods were exposed to the simulated groundwater flow for an insufficient amount of time to fully develop an indication of the flow direction.

A directional data analysis (Davis, 1986) was performed to statistically verify that the results of Test Nos. 2 through 6 had a preferred orientation for the vectors defined by the maximum fluorometer readings and their associated carbon rod locations (bearings). The results of Test No. 1 were omitted from the directional data analysis since the flow conditions were static. The calculation of the vector resultant for the experiments is presented in Table 2 and the equations that follow.

TABLE 2

DIRECTIONAL DATA ANALYSIS OF MAXIMUM FLUOROMETER READING VECTORS

Test No.	Maximum Fluorometer Reading	Vector Direction θ	Unit Vector End Point Coordinates	
			$X_i = \cos \theta_i$	$Y_i = \sin \theta_i$
2	0.025	270	0	-1
3	0.040	0	1	0
4	0.060	0	1	0
5	0.055	0	1	0
6	0.030	0	1	0
6	0.030	90	0	1

Note that there were two maximum fluorometer readings for Test No. 6; therefore, both values were included in Table 2. The length of the x and y components of the vector resultant were calculated using Eq. (2) and Eq. (3):

$$X_r = \sum_{i=1}^{n} \cos \theta_i = 4 \tag{2}$$

$$Y_r = \sum_{i=1}^{n} \sin \theta_i = 0 \tag{3}$$

The mean direction of the resultant vector, $\overline{\theta}$, which is the angular average of all the maximum fluorometer reading vectors in Test Nos. 2 through 6 was calculated by Eq. (4):

$$\overline{\theta} = \tan^{-1}\left(\frac{Y_r}{X_r}\right) = \tan^{-1}\left(\frac{0}{4}\right) = 0° \tag{4}$$

The resultant length is calculated using Eq. (5):

$$R = \sqrt{X_r^2 + Y_r^2} = \sqrt{4^2 + 0^2} = 4 \tag{5}$$

The mean resultant length, $\overline{R}$, is a measure of dispersion and is similar to the variance except that large values (approaching 1.0) indicate that the vectors are tightly bunched with a small dispersion while small values (approaching 0.0) indicate widely dispersed vectors. The mean resultant was calculated using Eq. (6) where n is the number of vectors:

$$\overline{R} = \frac{R}{n} = \frac{4}{6} = 0.67 \tag{6}$$

The mean resultant length calculated in Eq. (6) and the mean direction of the resultant vector calculated in Eq. (4) indicates that the maximum fluorometer reading vectors for Test Nos. 2 through 6 were fairly tightly bunched around the carbon rod at the 0º location. Therefore, the directional data analysis supported the conjecture that the fluorescein dye released into groundwater in a well and adsorbed onto carbon rods distributed around the inside perimeter of a well will indicate the direction of groundwater flow.

Additional statistical analysis was performed to determine whether the amount of fluorescein dye adsorbed onto the carbon rods as measured by the fluorometer in Test Nos. 1 through 6 was random (null hypothesis), as would be expected if there were no preferred groundwater flow direction, or nonrandom (alternate hypothesis) indicating a preferred groundwater flow direction. A goodness of fit analysis for the fluorometer readings was performed using the chi-squared (X^2) test (Chow et al., 1988). Eight intervals (m = 8) were used to evaluate the fluorometer readings representing the equal angle sectors of the horizontal circular plane of the well with a carbon rod located at the central bearing angle of each sector. The use of eight intervals (bins) assumed that fluorescein dye had an equal probability (P = 0.125) of flowing into any sector. For each experiment, the individual carbon rod fluorometer readings were expressed as percentages of the total fluorometer readings for the experiment. As a consequence of using the fluorometer readings expressed as percentages of the total fluorometer readings for an individual experiment and eight equal evaluation intervals (bins), the mean for each experiment was 12.5% as shown in Eq. (7):

$$\bar{x} = \frac{1}{n}\sum_{i=1}^{n} x_i = \frac{100\%}{8} = 12.5\% \tag{7}$$

where x_i is the fluorometer reading for a single carbon rod (rod number i) in the experiment expressed as a percentage of the total fluorometer readings for the experiment and n is the number (8) of carbon rods (evaluation intervals) in the experiment. The normalized square deviations, x_n, were determined using Eq. (8):

$$x_n = \frac{\left(x_i - \bar{x}\right)^2}{\bar{x}} \tag{8}$$

The computed X^2 for each experiment was found by summing the normalized square deviations, x_n. The X^2 calculations for each experiment are summarized in Table 3.

TABLE 3

SUMMARY OF X^2 CALCULATIONS FOR EACH FLOW DIRECTION TEST

Bin No.	Bin Interval	Fluorometer Reading	Fluorometer Readings as % of Total Readings x_i	Normalized Square Deviation x_n	Fluorometer Reading	Fluorometer Readings as % of Total Readings x_i	Normalized Square Deviation x_n
		Test No. 1			Test No. 2		
1	337.5º, 22.5º	0.030	15.385	0.666	0.020	14.815	0.429
2	22.5º, 67.5º	0.015	7.692	1.849	0.010	7.407	2.075
3	67.5º, 112.5º	0.020	10.256	0.403	0.015	11.111	0.154
4	112.5º, 157.5º	0.030	15.385	0.666	0.010	7.407	2.075
5	157.5º, 202.5º	0.030	15.385	0.666	0.020	14.815	0.429
6	202.5º, 247.5º	0.020	10.256	0.403	0.020	14.815	0.429
7	247.5º, 292.5º	0.030	15.385	0.666	0.025	18.519	2.898
8	292.5º, 337.5º	0.020	10.256	0.403	0.015	11.111	0.154
			Computed X^2	5.720		Computed X^2	8.642
		Test No. 3			Test No. 4		
1	337.5º, 22.5º	0.040	28.571	20.663	0.060	23.529	9.732
2	22.5º, 67.5º	0.020	14.286	0.255	0.040	15.686	0.812
3	67.5º, 112.5º	0.010	7.143	2.296	0.020	7.843	1.735
4	112.5º, 157.5º	0.010	7.143	2.296	0.025	9.804	0.582
5	157.5º, 202.5º	0.015	10.714	0.255	0.025	9.804	0.582
6	202.5º, 247.5º	0.015	10.714	0.255	0.035	13.725	0.120
7	247.5º, 292.5º	0.015	10.714	0.255	0.030	11.765	0.043
8	292.5º, 337.5º	0.015	10.714	0.255	0.020	7.843	1.735
			Computed X^2	26.531		Computed X^2	15.340
		Test No. 5			Test No. 6		
1	337.5º, 22.5º	0.055	18.644	3.020	0.030	18.182	2.583
2	22.5º, 67.5º	0.045	15.254	0.607	0.020	12.121	0.011
3	67.5º, 112.5º	0.030	10.169	0.435	0.030	18.182	2.583
4	112.5º, 157.5º	0.025	8.475	1.296	0.015	9.091	0.930
5	157.5º, 202.5º	0.030	10.169	0.435	0.010	6.061	3.317
6	202.5º, 247.5º	0.030	10.169	0.435	0.020	12.121	0.011
7	247.5º, 292.5º	0.035	11.864	0.032	0.015	9.091	0.930
8	292.5º, 337.5º	0.045	15.254	0.607	0.025	15.152	0.562
			Computed X^2	6.866		Computed X^2	10.927

The X^2 –distribution had ν degrees of freedom calculated by:

$$\nu = m - p - 1 \tag{9}$$

where m was the number of evaluation intervals (bins), in this case 8, and p was the number of evaluation parameters, in this case 1 ($\bar{x}$). The critical X^2 for $\nu = 6$ and $\alpha = 0.05$ (95% significance level) was found in a table of X^2 values to be 12.598 (Benjamin and Cornell, 1970). For test nos. 1, 2, 5, and 6, the critical X^2 value was higher than the computed X^2 values; therefore, the null hypothesis for the test (i.e. random distribution of fluorescein dye at the 95% significance level) cannot be rejected. These results should be expected for test nos. 1 (static flow conditions) and no. 2 (possible problem with carbon rod contamination by fluorescein dye stirred up by slow removal of the test device). Both test no. 5 and no. 6 had dominant fluorometer readings for the carbon rod at the 0º bearing location; however, there were also relatively large fluorometer readings at other carbon rod locations that resulted in the random dye distribution findings for the X^2 evaluation. For tests no. 3 and no. 4, the critical X^2 value was lower than the computed X^2 values; therefore, the alternative hypothesis (i.e. nonrandom distribution of fluorescein dye at the 95% significance level) cannot be rejected. Tests no. 3 and no. 4 demonstrated nonrandom distributions of fluorescein dye as detected by the fluorometer; therefore, it can be inferred that the test device measured the direction of flow in the well for these tests.

Groundwater Flow Velocity Results. The groundwater flow velocity measurement experiments were conducted in conjunction with and extended beyond the testing effort for the groundwater flow direction. Eight experiments were conducted, identified as Test Nos. 3 through 10 in Table 4. The flow velocities listed in Table 4 were determined using the continuity equation:

$$Q = V A \tag{10}$$

where Q is the discharge in ml/s, V is the average velocity in mm/s, and A is the cross-sectional flow area in mm^2. As mentioned earlier, the discharge was measured during each experiment by capturing water from the lower drain valve in the outlet standpipe in a graduated cylinder over a measured period of time. Therefore, the velocity of flow across the test section in the simulated well could be estimated from the velocity of flow in the horizontal pipe entering the simulated well. The horizontal pipe entering the simulated well had an inside diameter of 101.60 mm (4.00 inches) yielding a cross-section area of 8,107.32 mm^2 (12.57 in^2). Dividing the measured discharge by the cross-sectional area of the pipe entering the simulated well provided the mean cross-sectional velocity in the test section for each experiment.

Laminar flow conditions in the simulated well were confirmed by calculating the Reynolds number R for the velocities shown in Table 4 using the formula:

$$R = \frac{V D \rho}{\mu} \tag{11}$$

where V is the average velocity in m/s (ft/s), D is the pipe diameter in m (ft), ρ is the density of water in kg/m^3 ($slug/ft^3$), and μ is the absolute viscosity of water kg/m·s ($lb \cdot s/ft^2$) (Streeter and Wylie, 1975). For water temperatures during the experiments in the range 22ºC to 26ºC and the simulated groundwater velocities shown in Table 4, the Reynolds numbers were in the range of 0.03 to 0.05, which is well below the Reynolds lower critical number of 2,000; therefore, the simulated groundwater flow was laminar.

Table 4 summarizes the results of groundwater velocity measurement experiments including the fluorometer readings for the fluorescein dye/water mixture that remained in the dye release vial after each experiment.

TABLE 4

GROUNDWATER VELOCITY ANALYSIS FLUOROMETER RESULTS

Test No.	Time (min)	Flow (ml/s)	Velocity (mm/s)	Fluorometer Reading*
1	35	0.00	0.00E+00	---
2	60	3.37	4.15E-04	---
3	90	2.90	3.58E-04	22.00
4	30	2.17	2.67E-04	36.50
5	105	3.17	3.91E-04	38.00
6	20	2.67	3.29E-04	36.20
7	60	2.83	3.49E-04	35.50
8	105	2.57	3.17E-04	3.95
9	75	2.07	2.55E-04	33.80
10	50	2.17	2.67E-04	13.00

* A 1-m solution of fluorescein dye had a fluorometer reading of 44.20 at the beginning and end of the series of fluorometer tests.

The data in Table 4 introduces three variables, namely the time t, the groundwater discharge Q, and the fluorometer reading f. Note that the velocity V could easily replace the discharge Q since the cross-sectional area remained constant throughout the series of experiments. A multiple linear regression analysis of the data yields the relationship:

$$Q = -0.23t + 14.42f + 5.93 \tag{12}$$

with a multiple regression correlation coefficient (r^2) for this relationship of 0.55. While Eq. (12) does not provide a strong linear fit to the data, it does establish that the relationship between Q, f, and t can likely be represented as a series of parallel lines or curves similar to those shown on Figure 14, which is based on Eq. (12).

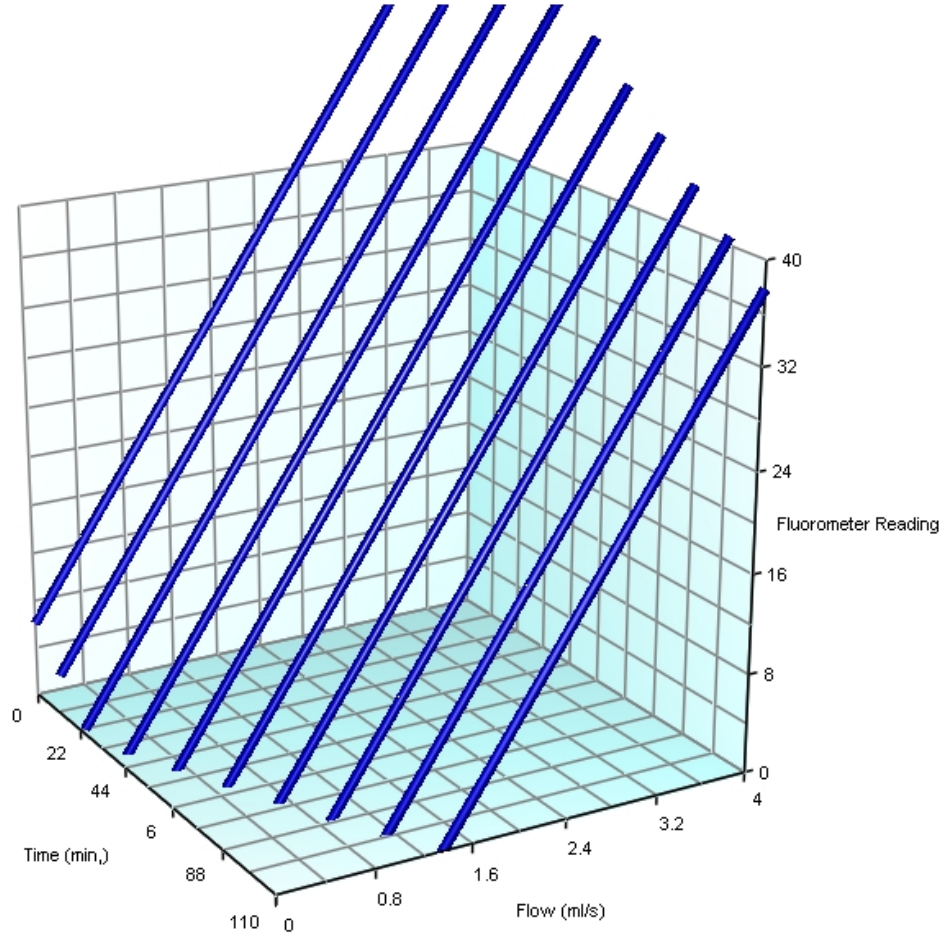

Fig. 14. Multiple-regression analysis results for the fluorescein dye concentration in the test release vial.

The relatively poor linear fit of the data in Table 4 can be explained by observations made during the experiments. The use of a salt plug release mechanism for the fluorescein dye was intended to provide sufficient time for any turbulence caused by the introduction of the groundwater flow direction and velocity measurement device into the simulated well to dissipate. However, the vertical saltwater density current caused by the dissolution of the salt plug and the flow of fluorescein dye may have introduced additional eddies in the groundwater flow. In addition, the point in time when the fluorescein dye began flowing from the hole in the modeling clay at the bottom of the dye release vial could not exactly be

determined. In several instances, fluorescein dye was observed accumulating atop the lower (stationary) polyethylene disk but could not be seen flowing from the dye release vial. In other experiments, the fluorescein dye appeared to be mixed with and entrained within the salt-water density current prior to the complete dissolution of the salt plug. The velocity measurement experiments were terminated when it became clear that a more precise dye release mechanism would be required to accurately measure the starting time for fluorescein dye discharge into the groundwater.

The use of a dissolving material, such as a salt plug, to control the release of fluorescein dye, introduces a number of uncertainties including the consistency of the salt, the uniformity of the salt plug geometry, and the uniformity of dissolution process. The effects of these uncertainties were directly observable through the window in the test apparatus. The salt-water density current sometimes flowed smoothly while at other times appeared to billow from the hole in the bottom of the modeling clay at the bottom of the dye release vial. On occasion, the salt plug appeared to disintegrate in pieces that fell through the salt water density current to the top of the lower (stationary) polyethylene disk.

An alternative analysis to determine the groundwater velocity was performed using the data in Table 1 and the root-mean-square (RMS) approach. The assumption in this approach was that the fluorescein dye adsorbed onto the carbon rods in each experiment would provide a measure of the groundwater flow velocity. The RMS for each experiment in Table 1 was calculated using the following equations:

$$\bar{x} = \frac{\sum_{i=1}^{n} x_i}{n} \tag{13}$$

$$r_i = \frac{x_i}{\bar{x}} \tag{14}$$

$$RMS = \sqrt{\frac{\sum_{i=1}^{n} (r_i - 1)^2}{n}} \tag{15}$$

where $\bar{x}$ was the mean of the fluorometer readings x_i, r_i was the ratio of the individual carbon rod fluorometer readings to the mean, and *RMS* is the root-mean-square of the fluorometer readings for an individual experiment. Table 5 summarizes the *RMS* calculations for the carbon rod data in Table 1. A linear regression analysis of the RMS and groundwater velocity data shown in Table 5 was performed and the results plotted, along with the actual data points, in Figure 15. There was weak correlation between groundwater velocity and the amount of fluorescein dye detected on the carbon rods in each experiment as indicated by the correlation coefficient (r^2) in Figure 15.

TABLE 5

GROUNDWATER FLOW VELOCITY ANALYSIS
USING ROOT-MEAN-SQUARES AND
CARBON ROD FLOUOROMETER RESULTS

Bearing (°)	Test No.											
	1		2		3		4		5		6	
	V =0.00E+00 mm/s t = 35 min.		V =4.15E-04 mm/s t = 60 min.		V =3.58E-04 mm/s t = 90 min.		V =2.67E-04 mm/s t = 30 min.		V =3.91E-04 mm/s t = 105 min.		V =3.29E-04 mm/s t = 20 min.	
	Reading x_i	r_i	Reading x_i	r_i	Reading x_i	r_i	Reading x_i	r_i	Reading x_i	r_i	Reading x_i	r_i
0	0.030	1.231	0.020	1.185	0.040	2.286	0.060	1.882	0.055	1.492	0.030	1.455
45	0.015	0.615	0.010	0.593	0.020	1.143	0.040	1.255	0.045	1.220	0.020	0.970
90	0.020	0.821	0.015	0.889	0.010	0.571	0.020	0.627	0.030	0.814	0.030	1.455
135	0.030	1.231	0.010	0.593	0.010	0.571	0.025	0.784	0.025	0.678	0.015	0.727
180	0.030	1.231	0.020	1.185	0.015	0.857	0.025	0.784	0.030	0.814	0.010	0.485
225	0.020	0.821	0.020	1.185	0.015	0.857	0.035	1.098	0.030	0.814	0.020	0.970
270	0.030	1.231	0.025	1.481	0.015	0.857	0.030	0.941	0.035	0.949	0.015	0.727
315	0.020	0.821	0.015	0.889	0.015	0.857	0.020	0.627	0.045	1.220	0.025	1.212
$\bar{x}$	0.024		0.017		0.018		0.032		0.037		0.021	
RMS	0.239		0.294		0.515		0.392		0.262		0.331	

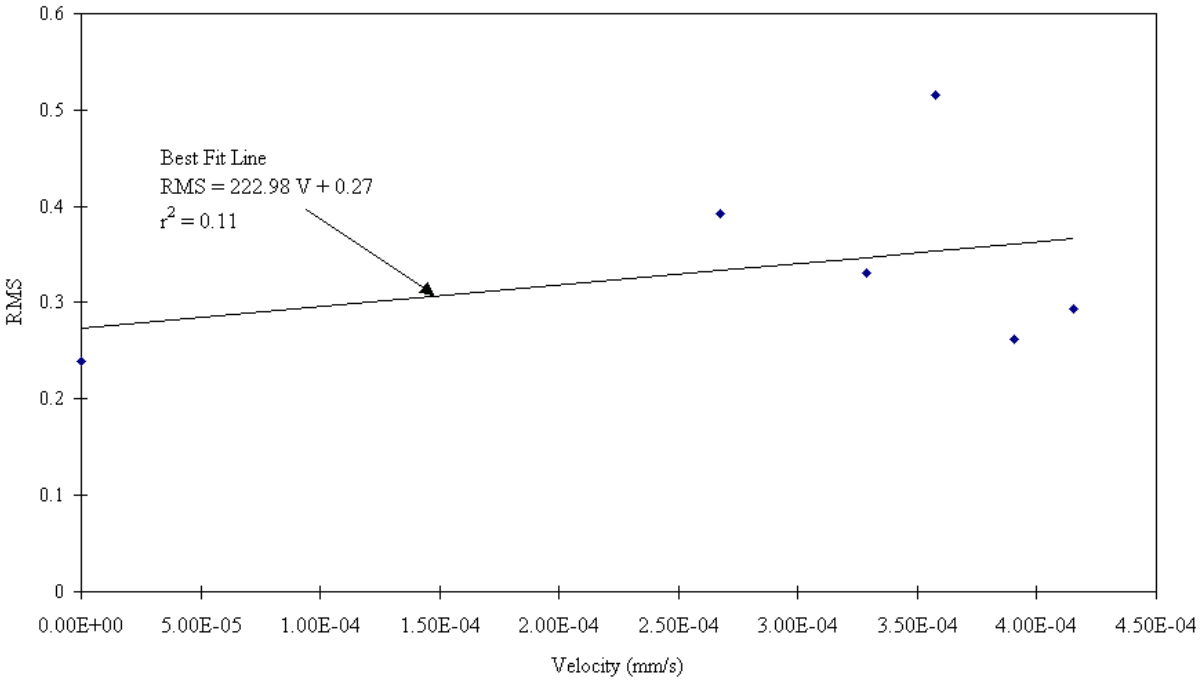

Fig. 15. Plot of RMS values derived from the carbon rod fluorometer readings versus groundwater velocity.

Conclusions

The experiments with the groundwater flow direction and velocity measurement device confirmed that carbon rods could be used to capture fluorescein dye entrained in groundwater flow. The rods were located at eight equally spaced intervals around the perimeter of a simulated well. An analysis of the amount of fluorescein dye captured by an individual carbon was performed by extracting the fluorescein dye from the carbon rod using methanol and then measuring the amount of the fluorescein dye present in the methanol using a fluorometer. The carbon rod most centrally located within the groundwater flow path in the simulated well adsorbed the highest amount of fluorescein dye. Thus the direction of flow could be determined from a comparison of the amount of fluorescein dye adsorbed by each of the carbon rods arranged around the well perimeter.

The evaluation of groundwater flow velocity using the groundwater flow direction and velocity measurement device developed for these experiments was less certain. An analysis of the groundwater flow, dye release time, and fluorometer readings for the fluorescein dye/groundwater solution remaining in the dye release vial led to a series of linear equations, based on a multiple linear regression, describing the groundwater flow in the form:

$$Q = J\,t + K\,f + L \tag{16}$$

where Q is the groundwater discharge, t is the time, f is the fluorometer reading, and J, K, and L are constants. The experiments to measure groundwater velocity were terminated when it was realized that the release time and rate of dye release in the groundwater flow direction and velocity measurement device could not be reliably observed or calibrated due to the inconsistencies of the salt plug dissolution process.

An alternative groundwater velocity analysis was also conducted using the root-mean-squares of the relative amounts of fluorescein dye extracted from all of the carbon rods from an individual experiment. A linear regression analysis of the data yielded the following equation:

$$RMS = 222.98\,V + 0.27 \tag{17}$$

where RMS is the root-mean-square of the fluorometer readings for the fluorescein dye extracted from the carbon rods for an individual experiment and V is the groundwater velocity. Equation (17) showed poor correlation (r^2) between the RMS values and V for the measured data.

It is suspected that the low Reynolds number laminar flow characteristics of the groundwater flow and the resulting turbulence caused by the introduction of a saltwater density current and fluorescein dye into the test section may be primarily responsible for the difficulty encountered in developing a relationship between groundwater velocity and the fluorometer readings for either the fluorescein dye/groundwater solution remaining in the dye release vial or the fluorescein dye adsorbed onto and extracted from the carbon rods. The vertical movement of the saltwater and fluorescein dye across the horizontal laminar

flow of the groundwater in the test section most certainly caused eddies to form that would affect the fluorescein dye/groundwater exchange process at the bottom of the dye release vial. The temperature difference between the groundwater and the fluorescein dye would also cause eddies to form due to changes in fluid densities as the dye flowed from the bottom of the dye release vial. The eddies would have regions of higher and lower fluorescein dye concentrations as they were swept past the carbon rods, which may partially explain why the maximum fluorometer reading for the carbon rods in one experiment may have a lower relative value than the maximum reading for another experiment conducted over less time. Eddies could have also been introduced by the interior configuration of the test apparatus and the measurement device, especially the joints between the pipes in the test apparatus. Eddies caused by the test apparatus would be analogous to those caused by a well screen. The possible impact of eddies caused by the introduction of a tracer, temperature differences, well configuration, or the measurement device calls into question the ability to directly and accurately measure groundwater velocity by any of the direct measurement techniques attempted by previous researchers.

The concerns with the affects of eddies on the accuracy of groundwater velocity measurements not withstanding, more accurate velocity measurements using fluorescein dye will require a more precise dye release mechanism. In actual applications, the groundwater flow direction and velocity measurement device would be suspended in a borehole where the moment of dye release could not be directly observed. A possible release mechanism could include a solenoid activated camera shutter type window or other thin physical barrier that could be slid to open a small hole to release the dye. However, the minimization of eddies caused by the mechanical opening of a shutter or barrier will need to be addressed in the design process.

Bibliography

Ballard, S. (1996). "The in situ permeable flow sensor: a ground-water flow velocity meter." *Ground Water.* 34(2), 231-240.

Ballard, S., G.T. Barker, and R.L. Nichols. (1996). "A test of the in situ permeable flow sensor at Savannah River, South Carolina." *Groundwater.* 34(3), 389-396.

Bardhan, M. (1975). "Investigation of vertical groundwater flow in boreholes." *Journal of Hydrology.* 25, 129-136.

Benjamin, J.R. and C.A. Cornell. (1970). *Probability, Statistics, and Decision for Civil Engineers.* McGraw-Hill Book Co. New York, NY.

Bredehoeft, J.D. and I. S. Papadopulos. (1965). "Rates of vertical groundwater movement estimated from the Earth's thermal profile." *Water Resources Research.* AGU. 1, 325-328.

Chow, V.T., D.R. Maidment, and L.W. Mays. (1988). *Applied Hydrology.* McGraw-Hill Publishing Co., New York, NY.

Davis, J.C. (1986). *Statistics and Data Analysis in Geology.* 2nd ed. John Wiley & Sons. New York, NY.

Drost, W., D. Klotz, A. Koch, H. Moser, F. Neumaier, and W. Rauert. (1968). "Point dilution methods of investigating ground water flow by means of radioisotopes." *Water Resources Research.* AGU. 4(1), 125-146.

Drury, M.J., A.M. Jessop, A.S. Judge, and T.J. Lewis. (1981). "The detection of groundwater flow by precise temperature measurements in boreholes." *EOS, Transactions.* AGU. 62(45), 864.

Freeze, R.A. and J.A. Cherry. (1979). *Groundwater.* Prentice-Hall, Englewood Cliffs, NJ.

Grisak, G.E., W.F. Merrit, and D.W. Williams. (1977). "A fluoride borehole dilution apparatus for groundwater velocity measurements." *Canadian Geotechnical Journal.* 14, 554-561.

Halevy, E., H. Moser, O. Zellhofer, and A. Zuber. (1967). "Borehole dilution techniques: a critical review." In: *Isotopes in Hydrology*. IAEA. Vienna. 531-564.

Hamada, H. (1999). "Estimation of groundwater flow rate using the decay of ^{222}Rn in a well." *Journal of Environmental Radioactivity.* Elsevier Science Ltd. 47, 1-13.

Hubbard, E.F., F.A. Kilpatrick, L.A. Martens, and J.F. Wilson, Jr. (1982). "Measurement of Time of Travel and Dispersion in Streams by Dye Tracing*." U.S. Geological Survey Techniques of Water-Resources Investigations*. Book 3, Chapter A9.

Kearl, P.M. (1997). "Observations of particle movement in a monitoring well using the colloidal borescope." *Journal of Hydrology.* Elsevier Science B.V. 200, 323-344.

Kerfoot, W.B. (1988). "Monitoring well construction and recommended procedures for direct ground-water flow measurements using a heat-pulsing flowmeter." In: Collins, A.G. and A.I. Johnson (Eds.), *Ground-Water Contamination: Field Methods.* ASTM. Philadelphia. 146-161.

Lu, N. and S. Ge. (1996). "Effects of horizontal heat and fluid flow on the vertical temperature distribution of a semiconducting layer." *Water Resources Research.* AGU. 32, 1449-1453.

Mansure, A.J. and M. Reiter. (1979). "A vertical ground-water movement correction for heat flow." *Journal of Geophysical Research.* 84, 3490-3496.

McCord, J., M. Reiter, and F. Phillips. (1992). "Heat flow data suggest large ground-water fluxes through Fruitland coals of the northern San Juan basin, Colorado-New Mexico." *Geology.* 20, 419-422.

Mizumura, K. and T. Hasatani. (2001). "Geochemical determinations of geological layers and groundwater flow directions." *Journal of Hydrologic Engineering.* ASCE. 6(3), 235-242.

Momii, K., K. Jinno, and F. Hirano. (1993). "Laboratory studies on a new laser doppler velocimeter system for horizontal groundwater velocity measurements in a borehole." *Water Resources Research.* AGU. 29(2), 283-291.

Mull, D.S., T.D. Liebermann, J.L. Smoot, and L.H. Woosley, Jr. (1988). *Application of Dye-Tracing Techniques for Determining Solute-Transport Characteristics of Ground Water in Karst Terranes.* EPA904/6-88-001. U.S. EPA. Atlanta, GA. 27-35.

Mull, D.S., J.L. Smoot, and T.D. Liebermann. (1988a). *Dye Tracing Techniques Used to Determine Ground-Water Flow in a Carbonate Aquifer System Near Elizabethtown, Kentucky.* USGS Water-Resources Investigations Report 87-4174. Lexington, KY.

Ochiai, T. (1964). "Measurement of groundwater velocity and its direction of flow by the use of radioisotope flow meter." in: *International Commission on Irrigation and Drainage, Annual Bulletin.*

Paillet, F.L., R.E. Crowder, and A.E. Hess. (1996). "High-resolution flowmeter logging applications with the heat-pulse flowmeter." *Journal of Environmental & Engineering Geophysics.* P.Carpenter ed. EEGS. 1(1), 1-11.

Peterson, R.E., E. Ballard, and S. Ballard. (1994). "In situ measurements of 3-D groundwater flow near the Columbia River, Hanford Site, Washington." *EOS, Transactions* . AGU. 75(44) Suppl. 276.

Quinlan, J.F. (1987). "Qualitative water-tracing with dyes in karst terranes." in: Quinlan, J.F., ed., *Practical Karst Hydrogeology, with Emphasis on Groundwater Modeling (course manual).* National Water Well Association. Dublin, OH. 6, E1-E24.

Reiter, M. (2001). "Using precision temperature logs to estimate horizontal and vertical groundwater flow components." *Water Resources Research.* AGU. 37, 663-674.

Reiter, M. and A.J. Mansure. (1983). "Geothermal studies in the San Juan Basin and Four Corners area of the Colorado Plateau, I, Terrestrial heat-flow measurements." *Tectonophysics.* 91, 233-251.

Reiter, M., J.K. Costain, and J. Minier. (1989). "Heat flow data and vertical groundwater movement, examples from southwestern Virginia." *Journal of Geophysical Research.* 94, 12423-12431.

Sébastien, L, J. Dighton, and W. Ullman. (2002). *Estimation of Groundwater Velocity in Riparian Zones Using Point Dilution Tests.* CSIRO Land and Water Technical Report 14/02. May. 1-16.

Stallman, R.W. (1963). "Computation of ground-water velocity from temperature data." *U.S. Geological Survey Water Supply Paper, 1544-H.* 36-46

Streeter, V.L. and E.B. Wylie. (1975). *Fluid Mechanics.* 6th Ed. McGraw-Hill Book Co. New York, NY.

"The First Fluorescent Dye Trace." (n.d.). Retrieved October 22, 2002, from Western Kentucky University, Center of Cave and Karst Studies Web site: http://www.dyetracing.com/dyetracing/dy01001.html

U.S. Department of Energy. (1998). *In Situ Permeable Flow Sensor.* OST Reference #99. Office of Environmental Management, Office of Science and Technology. Feb. 1-15.

Wheatcraft, S.W. (1986). "Measurement of hydraulic conductivity and groundwater velocity from a single borehole using a borehole thermal flowmeter." *EOS, Transactions.* AGU. 67(16), 276.

Yamada, K. and H. Arakawa. (1999). "Measurements of groundwater velocity by CCD camera in field observation wells and its vertical distribution." *Journal of Groundwater Hydrology.* Japanese Association of Groundwater Hydrology. 41(3), 193-201.